Cytotoxicity of Ashwagandha Derived Withaferin A to Human Cancer Cells : Molecular Insights into the Response of Telomerase Plus and Minus Cell

著者	于 躍
year	2016
その他のタイトル	アシュワガンダ由来ウィザフェリンAのヒト癌細胞に対する細胞毒性 : テロメラーゼ発現と非発現細胞の応答に対する分子洞察
学位授与大学	筑波大学 (University of Tsukuba)
学位授与年度	2016
報告番号	12102甲第7945号
URL	http://hdl.handle.net/2241/00145396

Cytotoxicity of Ashwagandha Derived Withaferin A to Human Cancer Cells: Molecular Insights into the Response of Telomerase Plus and Minus Cell

July 2016

Yue YU

Cytotoxicity of Ashwagandha Derived Withaferin A to Human Cancer Cells: Molecular Insights into the Response of Telomerase Plus and Minus Cell

A Dissertation Submitted to

Graduate School of Life and Environmental Sciences,

University of Tsukuba

in Partial Fulfillment of the Requirements

for the Degree of Doctor of Environmental Studides

(Doctoral Program in Sustainable Environmental Studies)

Yue YU

Abstract

Cancer is a complex disease, which is regulated by multifaceted network of signaling pathways driven by loss of activities of tumor suppressor proteins, gain of function of oncogenes and several epigenetic mechanisms. Being different from normal cells, cancer cells maintain telomere length to overcome replicative mortality by telomerase or alternative lengthening of telomeres (ALT) pathway. Disruption of either can induce DNA double-strand break signaling, leading to senescence or apoptosis. Significance of microRNAs (miRNAs), small non-coding molecules, has been also implicated in a variety of biological processes. miRNA expression correlates with various cancers, and these genes are thought to function as both tumour suppressors and oncogenes.

Withania somnifera (Ashwagandha), an important medicinal plant, is commonly known as “Indian ginseng” or “winter cherry”. It belongs to Solanaceae family and grows in dry regions of South Asia, Central Asia and Africa, particularly in India. It has been known to exert anti-tumor activity against various kinds of cancer. However, there is few study investigating the telomerase- or ALT-targeted potential of Withaferin-A (Wi-A) and the molecular mechanisms regulated by miRNAs.

Here, we used isogenic cells with or without telomerase and found that Wi-A caused stronger cytotoxity to ALT cells. The G_2/M arrest and apoptosis resulting from Wi-A exposure was specific to ALT cells. Treatment with Wi-A decreased in the number of ALT-associated promyelocytic leukemia (PML) nuclear bodies (APBs) (a universal characterization of ALT), whereas telomerase activity was unaffected. ALT cells treated with Wi-A exhibited severe telomere dysfunction and upregulation of DNA damage response. Molecular analysis revealed that treatment with Wi-A lead to Myc-mediated transcriptional suppression of MRN complex, which is essential for ALT mechanism and cell survival.

Meanwhile, we recruited arbitrary manipulation of genome and escape from 5-

Aza-2'-deoxycytidine (5-Aza-dC) induced senescence as a cell based loss-of-function screening system. Cells that escaped 5-Aza-dC induced senescence were recovered and subjected to miR-microarray analysis with respect to the untreated control. We identified miR-335 as one of the upregulated miRs implying that it is normally silenced by methylation. In order to characterize the functional significance, we overexpressed miR-335 in a variety of human cancer cells, with either telomerase or ALT mechanism, and found that it causes growth arrest and hence inhibited incorporation of 5-Aza-dC enabling cells to escape induction of senescence. We demonstrate that miR-335 targets multiple proteins including $p16^{INK4A}$, pRB and CARF (Collaborator of ARF) and causes growth arrest of cancer cells by complex interactions of its gene targets. Notably, miR-335 expression is increased by Wi-A treatment in telomerase cells, inducing CARF mediated cellular growth arrest.

Collectively, these results provide novel evidences for the anti-cancer property of Wi-A in the aspects of telomere maintenance and miRNA regulation. It provide a new strategy for the development of Wi-A based drug screening and designing in the future.

Keywords: cancer, telomere, cytotoxicity, senescence, microRNA

Contents

List of figures

Abbreviations

ARF	Alternate reading frame
ATM	Ataxia telangiectasia mutated
ATR	Ataxia telangiectasia and Rad 3 related protein
BSA	Bovine serum alibumin
CARF	Collaborator of ARF
CHK 1/2	Checkpoint kinase 1/2
CDKs	Cyclin dependent kinases
DDR	DNA damage response
DMEM	Dulbecc's modified eagle's medium
DMSO	Dimethyl sulfoxide
DNA	Deoxyribonucleic acid
DOX	Doxorubicin
ECL	Enhanced chemiluminescence
EDTA	Ethylenediaminetetraacetic acid
FBS	Fetal bovine serum
GFP	Green fluorescent protein
γH2AX	Gamma histone variant H2AX
HRP	Horseradish peroxidase
MDM2	mouse double minute 2
MTT	3-(4,5-dimethylthiazol-2-yl)-2,5-diphenyltetrazolium bromide
MRE11	Meiotic recombinnation 11
NBS1	Nijmegen breakage syndrome 1
PARP	Peroxisome proliferator activated receptor
PBS	Phosphate buffered saline
PCR	Polymerase chain reaction
PDs	Population doublings
PVDF	Poly vinylidene fluoride
RAD50	DNA repair protein 50

PI	Propidium iodide
Rb	Retinnoblastoma
RNA	Ribonucleic acid
ROS	Reactive oxygen sulfate
SDS	Sodium dodecyl sulfate
TRF2	Telomere repeat binding factor
Wi-A	Withaferin A
WS	*Withania somnifera*

Chapter 1 Introduction

1.1 Ashwagandha

Withania somnifera (Ashwagandha, WS), an important medicinal plant, is commonly known as “Indian ginseng” or “winter cherry” (Fig.1-1). It belongs to Solanaceae family and grows erectly with a normal height of 1.50 m. It is native in dry regions of South Asia, Central Asia and Africa, particularly in India. WS is cultivated on a commercial scale in India with the production of ~8000 tons (during 2005). The annual demand of this herb increased from ~7000 tons (2002) to ~9000 tons (2005).

For thousands of years, Ashwagandha is used for various kinds of disease protection and treatment in Indian traditional Ayurvedic system. It is applied as a general tonic that promotes a youthful state of physical and mental health and expands happiness. It is in use for a very long time for all age groups and both sexes and even during pregnancy without any side effects [1]. The extract is available over the counter in the United States as a dietary supplement. It is reported that the root can elevate human body’s resilience to stress by improving the cell-mediated immunity [2], and helping protect against cellular damage caused by free radicals [3]. The health benefit of Ashwaganda is supported by clinical trials in case of anti-inflammatory, anti-stress, anti-oxidant, anti-aging, anticonvulsant, anti-hyperglycaemic and anti-carcinogenic activities [4]. To date, over 35 chemical constituents have been discovered in WS. Among them, alkaloids, steroidal lactones and withanolides are believed to account for its extraordinary medicinal properties [5].

Withaferin A (Wi-A) is the first member of withanolides to be identified. Later on, chemical structure analysis suggests it is characterized by a closed ring consisting of 5 carbon atoms and a single oxygen atom [6]. Extensive studies indicate Wi-A possess inhibitory effect against several types of cancer, which is attributable to (i) induction of cell cycle arrest by downregulation of cyclin B1, cyclin A, Cdk2 and p-Cdc2 expression and an increase in the levels of p-Chk1 and p-Chk2, (ii) downregulation of expression

of HPV E6 and E7 oncoproteins, (iii) induction and accumulation of p53, (iv) increase levels of $p21^{WAF1}$, (v) decrease the levels of STAT3, (vi) increase in p53-mediated apoptotic markers-Bcl2, Bax, caspase-3, cleaved PARP and Par-4, (vii) and induced COX-2-mediated inflammatory response via miR-25 up-regulation [7-11]. In addition, Wi-A also suppresses metastasis via: (i) induction of Vimentin disassembly by ser56 phosphorylation, (ii) and downregulation of migration-promoting proteins hnRNP-K, VEGF, and metalloproteases [12, 13].

With our gain in knowledge of Wi-A, the therapeutic potential of WA seems very promising. However, the pharmacological and toxicological properties for human is still elusive. So large scale of pre-clinical studies need to be performed to eliminate any side effect in further clinical trials.

1.2 Telomere, telomerase and ALT

1.2.1 Telomere structure and function

Telomeres are long tracts of DNA at the linear chromosome's ends composed of successive TTAGGG repeats that vary in length from 2 to 20 kb [14]. Telomeric DNA is double stranded with a single – stranded terminus (G-tail) which is about 130-210 nucleotides (nt) in human cells. The ends of telomeres form a unique structure called a t-loop, which is formed by strand invasion of the 3' single strand overhang into the preceding double stranded telomeric DNA [15, 16]. Despite t-loop, the G-tail is also able to form a secondary four-strand structure named Gquadruplexes that can be either intermolecular or intramolecular [17]. As a result, such a structure may contribute to telomere stability and chromosome-end protection as they prohibit access of nucleases and DNA damage response (DDR) detection enzymes.

A six-protein complex known as "shelterin" has remarkable specificity for telomeres. Among of which, TRF1 and TRF2 bind directly to double stranded telomeric DNA, while the single-stranded tail is tied up by POT1. Furthermore, TRF2 recruits RAP1, and TIN2 can bridge TRF1 and the TRF2/RAP1 complex by binding to both

proteins simultaneously with different domains [18, 19]. TRF1 has been shown to promote telomere replication, thereby preventing telomeric damage [20]. TRF2 protect telomere from loss of 3' overhang and end to end fusion [21]. POT1 can regulate the telomerase essential to balance telomere elongation [22]. A careful analysis measuring the absolute and relative amounts of TRF1 and TRF2 in the nucleus revealed that TRF2 is about twice as abundant as TRF1 and subcomplexes of shelterin have been detected. Quantitation of other shelterin component showed the loading of POT1 is limited by the amount of TPP1 [23], suggesting shelterin components, in turn, are regulated by both the expression of coding genes and mutual modification that are growing-state specific. Moreover, shelterin components also have a key role in suppressing the ATM and ATR checkpoint pathways at telomeres. TRF2 can bind to and suppress ATM and POT1 inhibits ATR. Suppression of TRF2 activity elicits p53 and ATM activation, leading to telomere dysfunction induced foci (TIFs) [24, 25]. These considerations may widen our understanding of the roles of telomere in chromosome protection and genome integrity.

In the context of absence of any compensation mechanism, in most somatic cells of an adult organism, telomeres shorten during each cell division, resulting in cumulative telomere attrition. Consequently, after a finite number of cell divisions, telomeres reach a critical length and chromosomes become uncapped, leading to either permanent cell cycle arrest or to apoptosis [26-30]. Thus, telomeres act as a "clock" that determines lifespan at the cellular level. However, cancer cells are lacking of such regulatory mechnism due to the presence of telomerase or alternative lengthening of telomeres (ALT). To break the barrier of telomere attrition, about 85-90% cancer cells utilize telomerase to synthesizing new telomeric DNA repeats at chromosome ends [31], while the remaining 10-15% human cancers lacking detectable telomerase activity maintain telomere length by DNA recombination [32].

1.2.2 Telomerase

In most cases, telomerase activity is repressed in somatic cells, with the exception of adult stem cells, male sperm cells and renewal tissues [14]. It is, however, a universal

characterization of cancer cell lines. The human telomerase is a kind of ribonucleoprotein complex enzyme with action of copying the short RNA template sequence within the telomerase RNA into DNA. The complex mainly consisted of human telomerase reverse transcriptase (hTERT), and an associated template RNA called human Telomerase RNA (hTR or hTERC) [33-35]. hTR is ubiquitously expressed in all human cells, and telomerase activity is limited by the expression of hTERT, which is only found in telomerase positive cells. Introduction of hTERT into telomerase-silent cells is sufficient to reactivate telomerase, elongate or maintain telomeres [31, 36]. Besides these two core components, many other telomerase-associated proteins, for instance of dyskerin, are found and predicted to have an important role in telomerase recruitment, stabilization and regulation [37].

The distinct difference of telomerase expression between cancer and normal cells make telomerase a rational target for cancer therapeutics. Even though the intricacies of telomere function have not been fully elucidated, the clinical application of anti-telomerase therapies for cancer has been making rapid progress in the past 5-10 years. GRN163L is one of the first generation of oligonucleotide telomerase inhibitors for the treatment of cancer, and has entered Phase I/II clinical trials in patients with chronic lymphocytic leukaemia. Ongoing clinical trial results suggest it has the potential to be a universal anticancer agent with minimal side effects [38, 39]. In the aspect of gene therapy, an oncolytic virus named CG5757 is able to disrupt Rb and hTERT promoter region, proceeding to selectively kill the Rb-defective and hTERT-positive cancer cells [40-42]. Cells with peptides generated by degradation of hTERT can be recognized and killed by cytotoxic T-lymphocytes, which makes telomerase a potential target for immunotherapy. Telomerase-based universal cancer vaccines have been subjected to clinical trials and showed acceptable safety along with encouraging efficacy on tumor inhibition [43-45].

1.2.3 Alternative lengthening of telomeres (ALT)

Differing from telomerase, which uses an RNA template for telomeric DNA

synthesis, ALT generates new telomeric DNA from a DNA template via homologous recombination (HR). During cell replication, the relatively shorter telomere elongates itself by copying DNA sequence from: (i) another existing telomere at adjacent chromosome, (ii) another region from the same telomere through t-loop structure, (iii) the telomere of sister chromatid [32]. ALT-positive tumor or immortal cells are characterized by highly heterogeneous chromosomal telomere lengths; rapid changes in telomere length; an abundance of extrachromosomal telomeric DNA in the shape of double-stranded telomeric circles (t-circles) and single-stranded circles(C- or G-circles); and the presence of ALT-associated promyelocytic leukemia (PML) bodies (APBs) [46-50].

Genetic or epigenetic alterations that unleash ALT are remain unknown, but it has been believed that various HR proteins are involved. HR suppressing genes (p53, ATRX, DAXX and H3F3A) are found to be associated with ALT activation, and most of them affect chromatin remodeling at the telomere [51-54]. Early studies demonstrated suppression of HR related components, like MRN complex, SMC5/6 complex and BLM helicase, leads to telomere shortening, loss of APBs or alterations of other characteristics of ALT cell lines [55]. Compared to other immortalized cells, a large proportion of the telomeres in ALT cells evoke a DNA damage response, suggesting a high degree of ongoing genomic instability [56]. As a compensation, most of them possess a high level of DNA recombination events and defect in G2/M checkpoint [57, 58]. As a result, cells can keep on proliferating to overcome DNA damage. This dynamic process qualified ALT cells for dividing infinitely.

The MRE11-NBS1-RAD50 complex is the first proteins to be identified as necessary for ALT mediated telomere elongation [59]. It seems that this complex plays a dual role in telomere biology. Firstly, it functions in the detection and signaling double-strand breaks (DSB), further recruits ATM to break focis and facilitates 5’ to 3’ resection of the DNA ends to create 3’ overhangs for strand invasion [60]. Secondly, the MRN complex localizes to telomeres during the S and G2 phases of the cell cycle through

direct interaction of NBS1 with TRF2, contributing to G-tail stabilization [61, 62]. Furthermore, in telomerase expressing cells, MRN complex may also promote accessibility of telomerase to the 3' end of telomeres via TRF1 inhibition [63].

ALT has been detected in many tumor types but is most prevalent in tumors of mesenchymal origin like glioblastomas, osteosarcomas, soft tissue sarcomas, all of which tend to present particularly poor prognosis [64, 65]. Many molecular details of ALT remain to be discovered, however, and it is still possible to develop ALT-targeted therapeutic approaches for cancer treatment. Recent reports support this notion, as repression of ALT in ALT-dependent immortal cell lines resulted in selective senescence and cell death, while ALT inhibition by siRNA-targeting of ALT components appear to result in more rapid telomere dysfunction [66-68].

1.3 microRNAs

mircoRNAs (miRNAs) are non-coding, single-stranded RNAs of ~22 nucleotides and found in both plants and animals [69]. After their initial discovery in a study on *Caenor-habditis elegans* in 1993 [70], the development of research on this small sequence is very in the following decade. To date, over 2,500 potential human miRNAs are recorded in miRBase, a biological database that acts as an archive of miRNA sequences and annotations [71]. The predominant function of miRNAs is to negatively regulate the expression of target protein by binding to its coding sequence of messenger RNAs (mRNA). Mechanisms of action of miRNAs are mainly recognized in two different pathways depending on the level of complementarity between the miRNA and the target. First of all, in most of plants, miRNAs have been found to bind with perfect complementarity to protein coding mRNA sequences, resulting in mRNA degradation through RNA-mediated interference (RNAi) pathway [72, 73]. Nevertheless, vertebrate miRNAs are believed to use the other mechanism. Instead of the cleavage of their mRNA targets, these miRNAs inhibit target gene expression in post-transcription level by imperfect match to the 3' untranslated regions (UTRs) of target mRNA sequence [74-

[76]. In this case, the protein level of target genes is reduced, but mRNA level is barely affected. About one-third of human mRNAs are potentially controlled by miRNAs, because of the short microRNA–mRNA binding site which is commonly 6–8 base pairs. Each microRNA has the potential to target multiple different mRNAs, while a single mRNA may also have target sites for multiple microRNAs.

1.3.1 microRNAs biogenesis

The general biogenesis of miRNAs has already been elucidated. First, miRNA coding gene is transcribed by RNA polymerase II, generating long primary transcripts (pri-miRNAs). Subsequently, the RNase III–type enzyme (Drosha) processes the long primary transcripts into ~70-nucleotide hairpin precursors (pre-miRNA). The pre-miRNAs are then exported into the cytoplasm and undergo an additional processing step in which a double- stranded RNA of ~22 nucleotides duplex structures in length. Next, the less stable of the two strands in the duplex is incorporated into the miRNA-induced silencing complex (miRISC). The mature miRNA strand is preferentially retained in the functional miRISC complex and negatively regulates its target genes [77-81].

1.3.2 miroRNAs and cancer

miRNA expression correlates with various cancers, and these genes are thought to function as both tumor suppressors and oncogenes. The first indication of a link between microRNA deregulation and cancer has been uncovered in 2002. In this study, they found that B-cell chronic lymphocytic leukemia (CLL) often have deletions or downregulation of two clustered miRNA genes, mir-15a and mir-16-1 [82]. After this

first study a great number of microRNAs have been found deregulated in cancer. For example, mature miRNA levels of miR-143 and miR-145 are significantly reduced in colorectal tumors [83]. Another research indicated that miR-21 is 5-100-fold up-regulated in glioblastoma than normal tissue and knockdown of this miRNA in glioblastoma cell lines lead to apoptosis, which implies an oncogenic role for it [84].

miRNA-induced abnormal regulatory mechanisms are implicated in the pathogenesis of malignant tumors. Considering that loss of functional p53 is one of the most represented genetic abnormalities in cancer, the association of p53 and miRNA has been widely investigated. Accumulative studies revealed that [85]: (i) p53 promotes the Drosha-mediated processing and maturation of certain miRNAs with growth-suppressive function, including miR-16-1, miR-143 and miR-145. (ii)The transcription expression of numbers of miRNAs, including miR-34a/b/c, miR-145, miR-107, miR-192 and miR-215, are induced by p53. (iii) Some miRNAs are able to negatively regulate p53 function by direct binding to 3'UTR in mRNA, or positively regulate molecular antagonists of p53, like HDM2.

The differential expression of certain miRNAs has already been shown to be an accurate predictor of a patient's overall prognosis. Importantly, cancer-associated microRNA biomarkers can be detected in biological fluids, such as blood, urine and saliva, allowing less-invasive monitoring [86]. Isolation of exosomes from serum showed that a signature involving two microRNAs and one small non-coding RNA can be used for non-invasive diagnosis of glioblastoma [87]. The first microRNA-based therapy on clinical trial is MRX34: a synthetic miR-34a mimic loaded in liposomal nanoparticles. miR-34 inhibits multiple oncogenic pathways as well as stimulates anti-tumor immune response to induce cancer cell death. Introducing a mimic of miR-34 into cancer cell lines derived from patients with liver, lung, colon, pancreatic and breast cancers results in significant reductions in cell proliferation. Lipid-based local and systemic delivery of miR-34a in animal studies has also shown positive results for lung cancer [88-90].

Study on miRNAs provides us insight into the underlying mechanisms of oncogenesis, and offers a promising opportunity for cancer detection, diagnosis, and prognosis assessment.

1.4 Innovative point and structure of the thesis

This experimental study provided novel evidences for the anti-cancer property of Wi-A in the aspects of telomere maintenance and miRNA regulation. It indicated a new strategy for the development of Wi-A based drug screening and designing in the future

Chapter 1 Introduction

In this chapter, the background of this research was introduced, including Ashwagandha, telomerase, ALT and miRNA. Motivation and the structure of this study were also addressed.

Chapter 2 Withaferin-A exhibits stronger cytotoxicity to telomerase minus ALT cancer cells

In this chapter, Wi-A-induced phenotype(s) in TEP and ALT cells was clarified. A set of experiments were applied for exploring the underlying mechanism.

Chapter 3 Noncoding regulation of drug induced DNA damage signaling and cellular senescence in ALT cells

In this chapter, miR-335 was screened out. Its functional characterization and effect of Wi-A on miR-335 regulation were discussed as well.

Chapter 4 Conclusions and future researches

In this chapter, the main results are summarized. In particular, the future research points was also directed.

Fig. 1- 1 Ashwagandha plant

https://www.strictlymedicinalseeds.com/product.asp?specific=2784#

http://www.plantoftheweek.org/week194.shtml

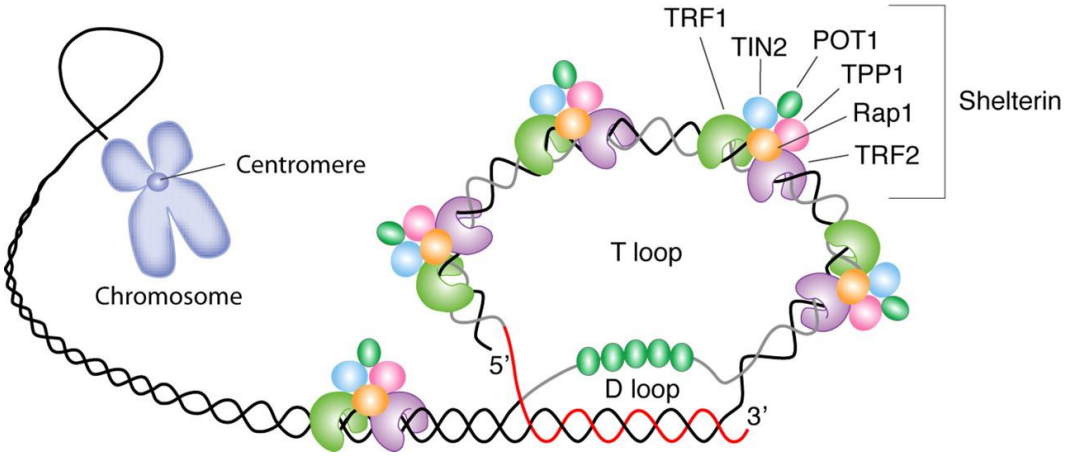

Fig. 1- 2 Schematic representation of telomere structure [91]

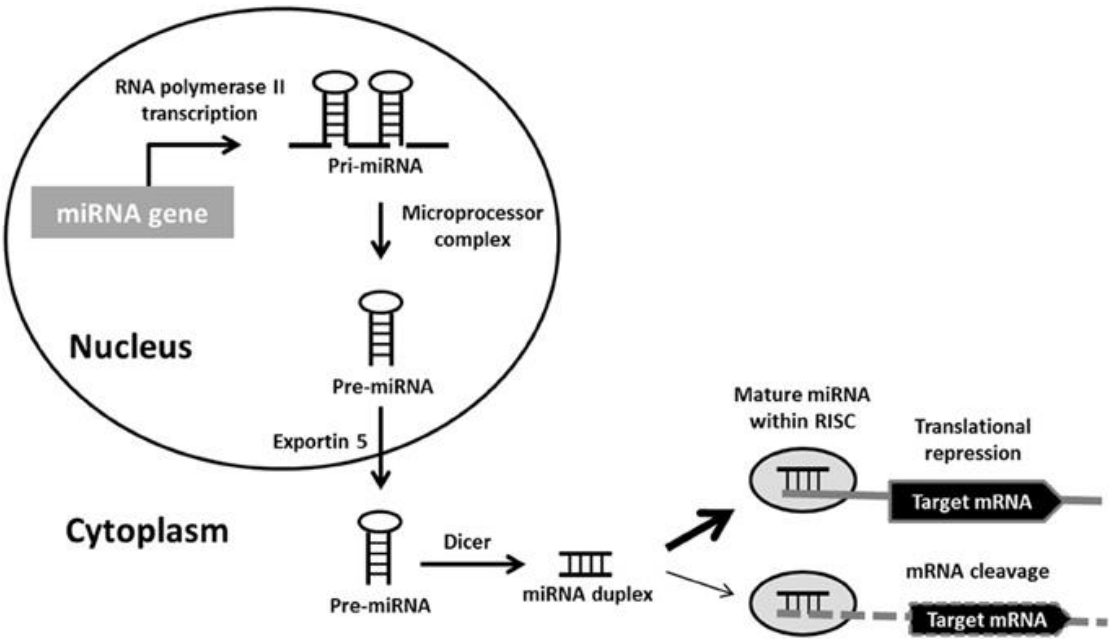

Fig. 1- 3 Model of microRNAs biogenesis [92]

Chapter 2 Withaferin-A exhibits stronger cytotoxicity to telomerase minus ALT cancer cells

2.1 Introduction

Normal somatic cells have a finite life span and undergo a permanent growth arrest called cellular senescence that acts as a strong tumor suppressor mechanism. It is regulated by telomere (chromosomal ends with tandem repeats of TTAGGG sequence) -shortening (an inherit DNA replication problem), and activity of tumor suppressor genes [93, 94]. While these characteristics of normal cells have been established as hallmarks of senescence, telomere length maintenance is essential for cellular immortalization, and carcinogenesis [95]. Cancer cells circumvent telomere shortening by activation of telomerase, a ribonucleoprotein consisting of RNA (TR) and reverse transcriptase enzyme (TERT) component that adds TTAGGG to telomeric ends and offsets the progressive loss of telomeres [96]. Ectopic expression of hTERT in normal human fibroblasts has been shown to induce elongation of telomeres, permanent cell proliferation and susceptibility to experimental transformation [97, 98]. In contrast to the large majority of cancer cells that maintain their telomeres by upregulation of telomerase, telomerase-negative cancer cells maintain their telomeres by mechanisms referred to as ALT (Alternate Lengthening of Telomeres). ALT cells are characterized by very heterogeneous telomeres and possess large donut-shaped nuclear structures (ALT-associated Promyelocytic Leukemia (PML) Body) called APB that contain telomeric DNA and several proteins including PML, TRF1, TRF2, Replication factor A, RAD51, RAD52 [47, 62, 99-102]. Reconstitution of telomerase activity in ALT cells has revealed that human cells are capable of utilizing telomerase- dependent and -independent mechanisms of telomere maintenance concomitantly [103, 104]. ALT has been detected not only in cultured cancer cells but also in the tumor tissues accounting for 10-15% of all cancers with high occurrence in astrocytomas and sarcomas [105-108].

The MRE11-RAD50-NBS1 (MRN) protein complex acts as a DNA damage

sensor and regulates signaling involved in DNA repair, cell cycle regulation, telomere maintenance and genome stability [109]. It regulates a number of kinases, like ATM (ataxia-telangiectasia mutated), ATR (ataxia-telangiectasia and Rad-3-related), and DNA PKcs (DNA protein kinase catalytic subunit) that control DNA damage-repair signaling and survival/growth arrest/apoptosis of cells in response to DNA damage [110-112]. MRN is essential for timely activation of ATM-mediated pathways [113]. The dysfunction of MRN elements has been associated with genome instability disorders including ataxia telangiectasia (A-T), A-T-like disorder (ATLD) and Nijmegen breakage syndrome (NBS1). The latter is an autosomal genetic disease leading to premature aging, rapid telomere shortening, increased cancer incidence, chromosome instability, and sensitivity to ionizing radiation [114]. NBS1 plays a critical role in DNA damage response and the preservation of chromosomal integrity [115]. Whereas overexpression of NBS1 was shown to increase cell proliferation [116], its knockdown led to hypermutability and telomere changes that have been related to cancer predisposition in NBS disease [117]. Hypomorphic mutations MRE11 gene lead to A-T like disease (A-TLD) [118]. Cells compromised for Rad50 also showed rapid shortening of chromosome ends and their fusions [119, 120]. siRNA-mediated depletion of any of the subunits of MRN complex led to ablation of other subunits of the complex suggesting their co-regulation [59, 121, 122]. Overexpression of Sp100 that held the MRE11, RAD50, and NBS1 proteins away from APBs resulted in repression of the ALT mechanism including telomere length changes, and suppression of APB formation [55] suggesting that MRN is involved in ALT mechanism(s) of telomere maintenance.

It has been shown that MYCN transcriptionally control the expression of each component of the MRN complex that is required for MYCN-dependent proliferation [123]. c-Myc was shown to directly activate NBS1 and its function in DSB repair pathway [116]. c-Myc overexpression caused telomerase reactivation and telomere stabilization leading to continued proliferation of cells [97]. These results indicated that NBS1 is a direct transcriptional target of c-Myc and links the function of c-Myc to the

regulation of DNA-DSB repair pathway [116]. Consistent with the telomerase activation in cancer, anti-telomerase drugs are trusted as potent anti-cancer therapeutics. However, ALT tumors would be refractory to these drugs and hence urge the need of identification and characterization of new anti-ALT drugs.

In this study, we used unique isogenic cells with/without telomerase and investigated the anticancer potential role of Wi-A on telomere maintenance mechanism.

2.2 Materials and methods

2.2.1 Preparation of Withaferin A

Withaferin A (Wi-A) was prepared from the dried Ashwagandha leaves, as described previously [124]. Integrity of the preparation was determined by HPLC and NMR analysis as described [124]. Stock of Wi-A (10 mM) were prepared in DMSO and stored in -20℃. Working concentrations of Wi-A were prepared in cell culture medium.

2.2.2 Cell culture, treatments and viability assays

Human normal fibroblasts (MRC5), breast carcinoma (MCF7) and melanoma (G361) were obtained from Japanese Collection of Research Bioresources (JCRB, Japan). SV40-immortalized human fibroblast lines (JFCF-6/T.1J/6B and JFCF-6/T.1J/6G (telomerase), JFCF-6/T.1L and JFCF-6/T.1J/1-4D (ALT)) were generated in the laboratory of Dr. Reddel. All the four cell lines were subclones from the same transformation event as described earlier [125-127]. MRC5-hTERT was a kind gift from Dr. Reddel as well. Cells were cultured in Dulbecco's modified Eagle's medium (DMEM; Gibco BRL, Grand Island, NY, USA) supplemented with 10%(v/v) fetal bovine serum (Gibco BRL), and 1%(v/v) penicillin/streptomycin in the presence of 5% CO_2 at 37℃. Cells were treated with Wi-A at about 60% confluency. Morphological observations were recorded by phase contrast microscope (Nikon Eclipse TE300, Japan). The plates were stained with Crystal Violet and scanned for records. Cell viability was determined by MTT assay (Life technologies, Carlsbad, CA, USA) following manufacturer's instructions. Briefly, cells after the treatment with Wi-A for

24-48 h were incubated with MTT (0.5 mg/mL) for 4 h at 37℃ followed by replacement of MTT containing medium with 100 µl DMSO to dissolve formazan crystals. Plates were then read on a microplate reader (infinite M200 PRO, TECAN, Switzerland) at 570 nm. For long-term cell viability and proliferation, colony-forming assay was performed. 500 cells were plated in a 6-well plate and treated with Wi-A for 6 h. Then cells were left to form colonies for the next 10-15 days with a regular change of medium on every third day. Colonies were fixed with pre-chilled methanol/acetone (1/1, v/v) 10 min on ice, stained with 0.1% crystal violet solution, photographed and counted.

2.2.3 Antibodies

The following antibodies were used in this study: rabbit anti-PARP-1(H-250), anti-caspase-3(H-277) and anti-POT1(H-200) (Santa Cruz, CA, USA); goat anti-PML(N-19) (Santa Cruz); mouse anti-p53(DO-1), anti-Cyclin B1(GNS1), anti-N-myc and anti-TRF2(4A794) (Santa Cruz); rabbit anti-c-Myc(Y69) anti-PARP-9 and anti-PML(Abcam, Cambridge, MA, USA); mouse anti-Rad50(13B3/2C6), anti-Mre11(12D7) and anti-NBS1(NBS1-501) (Abcam); rabbit anti-phospho-histone H2A.X(20E3) and anti-Rad50(Cell Signaling, MA, USA); Mouse anti-TRF2(Cell Signaling); mouse anti-phospho-histone H2A.X(Millipore, Billerica, MA, USA); and rabbit anti-NBS1(Novus, Cambridge, UK). Anti-beta Actin antibody (AC-15) (Abcam) was used as an internal loading control.

2.2.4 Flow cytometry analysis

For the cell cycle analysis, cells were harvested by trypsin. Cell pellets were washed with cold PBS followed by addition of cold 70% ethanol drop-wise and incubated at at 4℃ overnight. The fixed cells were centrifuged at 800g for 5 min at 4℃, washed with cold PBS twice and then re-suspended in 0.25 ml PBS. The cells suspensions were treated with RNase A at 37℃ for 1 hour followed by brief centrifugation to discard supernatant. Cells were re-suspended in 200 µl of Cell Cycle

Guava reagent (Millipore, Billerica, MA, USA), incubated for 30 min in dark, and analyzed by EasyCyte Guava cytometer (Millipore). The data were further analyzed using FlowJo software (version 7.6, Flow Jo, LLC., USA).

For detection of apoptosis, WA treated attached and suspended cells were collected. Cells were suspended in 100 µl of medium and incubated together with 100 µl of Guava Nexin Reagent, a pre-made cocktail containing Annexin V-PE and 7-AAD, in a final volume of 200 µl and incubated for 20 minutes at room temperature in the dark. Samples then were measured on EasyCyte Guava cytometer (Millipore) and analyzed using FlowJo software.

2.2.5 Luciferase reporter assay

PG13-luc (wt p53 binding sites) was a gift from Bert Vogelstein (Addgene plasmid # 16442). Cells were cultured in 6-well plate, co-transfected with 1 µg of luciferase constructs (PG13-luc) and 100 ng of control vector oligonucleotide (pRL-TK using Lipofectamine 2000 (Invitrogen, Carlsbad, CA, USA). After 24-48 h, luciferase activity was measured using a dual luciferase reporter assay system (Promega, Madison, WI, USA) following the manufacturer's protocol. Experiments were carried out in triplicate and repeated at least three times.

2.2.6 Comet assay

DNA double-strand breaks were quantitated by a Comet assay system (Trevigen, Inc, Gaithersburg, MD, USA) according to the manufacturer's recommendations. Briefly, JFCF-6B and JFCF-1L cells were treated with or without WA for 24 h before mixing with low-melting point agarose and applied onto the CometSlide (Trevigen). Cells on the slides were lysed with prechilled lysis solution and incubated with neutral unwinding solution. Samples were then subjected to electrophoresis in cold neutral electrophoresis solution at 21 V for 30 min. Slides were washed twice with water and 70% ethanol and air dried before the addition of Gel Green solution (Biotium, Hayward, CA, USA). At least 200 cells on each slide were randomly selected for analysis using

Carl Zeiss microscope (Axiovert 200 M, Tokyo, Japan) with epifluorescence optics. The extent of DNA damage was calculated and showed as percent DNA in the tail using the OpenComet (v1.3), a plugin for the image processing program ImageJ. The study was repeated independently three times. The data are displayed as a box and whisker diagram showing median and middle quartiles with whiskers at the min and max.

2.2.7 Immunofluorescence

Cells were plated on a glass coverslip placed in a 12-well culture dish. After 24 h, when cells had attached well to the dish, they were washed with cold PBS and fixed with pre-chilled methanol/acetone (1/1, v/v) mixture or 4% paraformaldehyde for 10 min. Fixed cells were washed with PBS, permeabilized with 0.5% Triton X-100 in PBS for 10 min and blocked with 0.2% BSA/PBS for 1 h. Cells were incubated with appropriate antibody described above at 4°C overnight, washed thrice with 0.2% Triton X-100 in PBS, and then incubated with Alexa-594/488-conjugated goat anti-mouse or anti-rabbit (Molecular Probes, Invitrogen) secondary antibodies. Finally cells were counterstained with or without Hoechst 33342 (Sigma) for 10 min in dark. After extensive washings with 0.2% Triton X-100 in PBS, cells were mounted and stored at 4°C for microscope analysis.

The Telomere dysfunction induced foci (TIF) assay based on the co-localization detection of DNA damage markers (γH_2AX) and telomeric protein (TRF1 or TRF2) was performed as described [128]. APBs detection (double staining of telomere shelterin proteins, such as TRF2 and APB-associated protein such as PML) was performed as described [125]. Stained samples were examined on a Zeiss Axiovert 200M microscope and analyzed by AxioVision 4.6 software (Carl Zeiss). At least 200 cells (on duplicate slides) were evaluated for each treatment condition for co-localization foci counting. Images were quantified by ImageJ software (National Institute of Health, Bethesda, MD).

2.2.8 Western Blotting

Cells were lysed with radioimmunoprecipitation assay buffer (Thermo Scientific) containing complete protease inhibitor cocktail (Roche Applied Science, Mannheim, Germany). Cell lysates were separated on a SDS-polyacrylamide gel and transferred onto PVDF membranes. After probing with the primary antibody as indicated, the blots were incubated with horseradish peroxidase-conjugated goat anti-mouse or anti-rabbit antibodies (Santa Cruz) and detected using ECL substrate (Amersham Pharmacia Biotech/GE Healthcare, Piscataway, NJ, USA). Densitometric quantitation of the representative immunoblots was carried out using the ImageJ software (National Institute of Health). All the experiments were performed in triplicate at least three times.

2.2.9 RNA extraction and real-time qRT–PCR

Total RNA was isolated from cells using the RNeasy mini kit (Qiagen, Standford Valencia,CA, USA). The concentration and purity of RNA were determined by ultraviolet spectrophotometry (A260/A280 >1.9) using NanoDrop ND-1000 (Nanodrop Technologies, Wilmington, DE, USA). Equal amount of RNA were used for reverse transcription following the protocol of QuantiTect Rev. Transcription Kit (Qiagen). The real-time qRT–PCR was performed using SYBR® Select Master Mix (Applied Biosystems). The qPCR oligonucleotide primers sets were described as follow: NBS1 sense (5'-aagaagatacatgggatttgagtg-3'), NBS1 antisense (5'-tggagactttgatttgatttcttttggc-3'); MRE11 sense (5'-gccttcccgaaatgtcacta-3'), MRE11 antisense (5'-ttcaaaatcaacccctttcg-3'); RAD50 sense (5'-gaattatccactgaagttcagt-3'), RAD50 antisense (5'-tccaaagggcttacctgctc-3'); 18S sense (5'-cagggttcgattccgtagag-3'), 18S antisense (5'-cctccagtggatcctcgtta-3'). qRT-PCR reaction was carried out in triplicate on the Eco™ real time system (Illumina, San Diego, CA USA). The results were analyzed and expressed as relative expression of threshold cycle value, which was then converted to x-fold changes ($2^{-\Delta\Delta Ct}$).

2.2.10 TRAP assay

Telomerase activity was determined with a PCR-based telomeric repeat amplification protocol (TRAP) enzyme-linked immunosorbent assay (ELISA) kit (Roche, Mannheim, Germany) according to the manufacturer's protocol. In brief, cells were collected 24/48 h after treatment. The cells were washed three times with cold PBS, homogenized in 200 µl cell lysis buffer, and incubated on ice for 30 min. For the TRAP reaction, 10 µg of cell extract was added to 25 µl of reaction mixture, and sterile water was added to a final volume of 50 µl. PCR was then performed as follows: primer elongation (30min, 25°C), telomerase inactivation (5 min, 94°C), product amplification for 30 cycles (94°C for 30 sec, 50°C for 30 sec, and 72°C for 90 sec) and then balance (10 min at 72°C). A total of 5 µl of PCR products was added to a streptavidin-coated 96-well plate and hybridized to a digoxigenin (DIG)-labeled telomeric repeat-specific detection probe. The immobilized PCR products were detected with peroxidise-conjugated anti-DIG antibody. After addition of the stop reagent, the plate was assessed with a plate reader at a wavelength of 450 nm within 30 min.

2.2.11 Statistical analysis

All experiments were carried out in triplicates, and data were expressed as mean ± standard deviation (SD). Two-tailed Student’s t-test or nonparametric ManneWhitney U-test, whichever was applicable, was used to determine the degree of significance between the control and experimental sample. Statistical significance was defined as p-value ≤ 0.05.

2.3 Results and discussion

2.3.1 Withaferin A causes stronger cytotoxicity to ALT cells

We used isogenic cells with and without telomerase for cytotoxicity assays in response to Withaferin-A. As shown in Figs. 2-1A - 1C, dose-dependent cytotoxic response was observed for all the four cell lines (Telomerase Plus-TEP and telomerase

negative, ALT). Of note, ALT (JFCF-1L and 4D) cells showed stronger cytotoxicity at all doses as compared to the Telomerase Plus (TEP; JFCF-6B and 6G) cells. The IC_{50} values for 24h treatment were 0.6 μg/ml (JFCF-4D) and 0.9μg/ml (JFCF-1L) for ALT, and 1.2 μg/ml (JFCF-6B) and 1.4 μg/ml (JFCF-6G) for TEP cells. For 48 h treatment, IC_{50} values were 0.19 μg/ml (JFCF-4D), 0.25 μg/ml (JFCF-1L) for ALT, and 0.44 μg/ml (JFCF-6B) and 0.5 μg/ml (JFCF-6G) for TEP cells. The results were confirmed by visual observations that showed that whereas ALT cells underwent apoptosis at 0.5 and 1 ug/ml Wi-A, TEP cells were not affected (Fig. 2-2A). In line with these observations, long–term survival (colony forming assays) with low doses (0.25 μg/ml) of Wi-A showed that Wi-A caused stronger cytotoxicity to ALT cells as compared to the TEP cells (Fig. 2-2B).

2.3.2 Withaferin A caused stronger G_2-M arrest and apoptosis of ALT cells

Anti-proliferative effect of many natural chemotherapeutic agents is highly related to their ability to cause growth arrest or apoptosis [11, 129-132]. To determine whether cytotoxicity of Wi-A to ALT and TEP cells was due to the induction of growth arrest/apoptosis, we next performed cell cycle analysis on control and Wi-A treated cells. As shown in Figs. 2-3A and 3B, Wi-A treated ALT cells showed significant increase in the number of cells in G_2/M phase. Of note, equivalent doses did not cause similar G_2/M arrest in TEP cells. Furthermore, the treatment with Wi-A led to dramatic induction of apoptosis in ALT (JFCF-1L), but not in TEP (JFCF-6B) cells (Figs. 2-4A and 4B).

In order to get molecular insights to the apoptotic phenotype induced by Wi-A, we examined the expression level of pivotal proteins associated with apoptosis and G_2/M transition by Western Blotting. As shown in Figs. 2-5A and 5B, we found that, in the ALT cells, Wi-A treatment caused a marked increase in the cleaved PAPR-1 and PARP-9 (established makers of apoptosis). Consistent with this, total PARP-1/9 showed decrease in Wi-A treated ALT cells. In contrast, no significant change was observed in Wi-A treated TEP (JFCF-6B) cells. Similar to the change in PARP-1/9 that endorsed

occurrence of apoptosis in Wi-A treated ALT cells, procaspase-3 showed decrease in ALT, but not in TEP cells treated with equivalent dose (0.5 μg/ml) of Wi-A (Fig. 2-5C).

We next examined p53 and Cyclin B1, the two key regulators of cell cycle progression. As shown Fig. 2-6A, both ALT (JFCF-1L) and TEP (JFCF-6B) cells did not show wild type p53 activity as determined by wild type p53-dependent reporter assay. Western blotting for p53 in control and Wi-A treated cells revealed its down-regulation in ALT cells; TEP plus cells did not show such decrease in mutant p53 (Fig. 2-6B). Similar to the effect of Wi-A on p53, Cyclin B1 showed decrease in Wi-A treated ALT cells only. TEP cells, on the other hand, showed small/moderate increase in Cyclin B1 (Fig. 2-6B). Taken together, these data suggested that stronger toxicity of Wi-A to ALT cells is mediated by induction of apoptotic signaling.

2.3.3 Withaferin A causes the phenotype inhibition of ALT, but not that of telomerase

Given the above findings that Wi-A caused stronger cytotoxicity to ALT cells, we investigated the possibility of the effect of Wi-A on ALT mechanism involved in immortalization process of these cells. We examined a well-established marker (APBs formation) of ALT cells by visualizing co-localization of TRF2 (telomeric binding protein) and PML bodies. As shown in Fig. 2-7A, we detected APBs selectively in ALT cells. Of note, Wi-A treated ALT cells showed reduction in APBs by 20-40 % reduction in several independent experiments (Fig. 2-7B). To test the effect of Wi-A on telomerase activity, we performed TRAP assay in TEP (JFCF-6B, MCF7 and G361) cells. However, Wi-A treated TEP cells did not show any inhibition of telomerase activity (Fig. 2-8A). In order to further rule out the effect of Wi-A on telomerase, we used normal human fibroblasts (MRC5) and their hTERT-derivatives. As shown in Fig. 2-8B, these cells showed similar response to Wi-A suggesting that telomerase is not a direct target of Wi-A cytotoxicity to TEP cells. Taken together, Wi-A caused inhibition of ALT mechanism and hence caused stronger cytotoxicity to ALT cells.

2.3.4 Withaferin A causes stronger upregulation of DNA damage response in ALT cells

We next performed neutral Comet assay for measuring DNA double strand breaks (DSB) directly. As the data shown in Fig. 2-9A and 9B, a marked (2-fold) increase in DSB formation was observed in ALT cells exposed to Wi-A. On the other hand, DNA percent in tail of Wi-A treated TEP (JFCF-6B) cells showed no difference with respect to the control group suggesting that these cells are somewhat resistant to Wi-A induced DSB. The induction of DNA breaks after Wi-A treatment was also assayed by γH2AX immunostaining. Whereas JFCF-6B cells showed no difference in γH2AX staining between control and Wi-A (0.25 ug/ml) treated cells, JFCF-1L cells showed large increase in the number of γH2AX positive cells (Fig. 2-9A and 9C). These data were consistent with Comet assay data showed above and suggested that Wi-A caused stronger DNA Damage response in ALT cells.

To ascertain whether Wi-A treatment lead to telomere de-protection, we measured the number of cells with telomere-dysfunction-induced foci (TIF) by co-localization of γH2AX and TRF2 signals in control and Wi-A treated (Fig. 2-10A). We found that Wi-A increased the number of TIF-positive cells (TIFs ≥4) from ~10% up to ~25% in ALT (JFCF-1L) cells (Fig. 2-10B). In contrast to the induction of telomere damage by Wi-A in ALT cells, TEP (JFCF-6B) cells showed no significant difference in telomeric DNA damage under the same conditions (Fig. 2-10A and 10B).

Several studies have provided evidence that telomere binding proteins TRF2 and POT1 are predominantly involved in chromosome end protection by preventing DNA damage activation [133] [134]. In view of these reports and our above findings, we considered whether Wi-A targets TRF2 and POT1. Western blots for these proteins revealed down-regulation of both TRF2 and POT1 in Wi-A treated ALT cells; TEP cells showed lower level of expression that was not altered by Wi-A treatment (Fig. 2-11A and 11B). These data suggested that stronger cytotoxicity of Wi-A to ALT cells is due to, at least in part, its effect on ALT mechanism enriched in these cells.

2.3.5 MRN complex is involved in Wi-A caused DNA damage

Based on the above data that suggested targeting of ALT mechanism by Wi-A, we investigated MRN complex proteins that are essential for ALT mechanism and APB assembly [59, 135]. Western blotting with specific antibodies in control and Wi-A treated cells revealed a sharp decrease of NBS1 and MRE11 and relative less reduction of RAD50 in the latter (Fig. 2-12A and 12C). TEP cells showed only a small/negligible change (Fig. 2-12A and 12C). We also performed real-time PCR for their transcripts and found reduction in NBS1, but not in MRE11 and RAD50 in ALT cells. Rather, a slight increase was observed in MRE11 and RAD50 in Wi-A treated cells. TEP cells also showed a small increase in RAD50 (Fig. 2-12B). Since MRN complex is regulated by n-myc and c-myc [116], we next performed Western blotting for myc proteins expression in control and Wi-A treated ALT and TEP cells. Of note, Wi-A led to significant decrease of both in JFCF-1L, while myc expressions in JFCF-6B treated cells were barely changed (Fig. 2-12A). Consequently, we concluded that Wi-A caused down-regulation of MRN complex proteins in ALT cells through the inhibition of their transcriptional factor n-myc/c-myc.

DNA damage is an inherit phenomenon that occurs with DNA replication and several other functions of cells that are essential for cell survival. Cells possess built-in DNA damage sensing and repair mechanisms constituted of MRN-ATM/ATR-p53-p21 signaling [113, 118, 136]. Telomere shortening has been established to evoke DNA damage response that initiates senescence and apoptosis to avoid tumorigenesis [98]. Cancer cells escape from telomere shortening by mechanism(s) involving either telomerase or ALT [137]. Both of these have been considered as drug targets for cancer therapy. More efforts have been focused on the telomerase inhibitors due to high incidence (80-90%) of telomerase activation as compared to (10-20%). The presence of ALT is more common and associated with decreased clinical outcome than telomerase mechanism in astrocytomas and glioblastomas and fibrous histiocytomas, liposarcomas. Hence, the drugs effective for ALT cells are important and valuable for cancer treatment. Recently,

an ATR inhibitor, VE-821 was shown to cause ALT stronger DNA damage to ALT cancer cells [138]. *In vitro* studies have demonstrated that telomerase and ALT mechanism can co-exist within individual cell. Inhibition of TEP could activate ALT or vice versa [139] raising the need for dual action inhibitors. Wi-A could serve as one of such promising candidate drug.

2.4 Summary

We found that Wi-A caused stronger cytotoxity to ALT cells. It was associated with ALT-associated promyelocytic leukemia (PML) nuclear bodies (APBs), an established marker of ALT. Comparative analyses of telomerase positive and ALT cells revealed that Wi-A caused stronger telomere dysfunction and upregulation of DNA damage response in ALT cells. Molecular analyses revealed that the treatment with Wi-A lead to c-Myc- and n-Myc-mediated transcriptional suppression of MRN complex, an essential component of ALT mechanism. The results suggest that Wi-A may be a new candidate drug for ALT cancers.

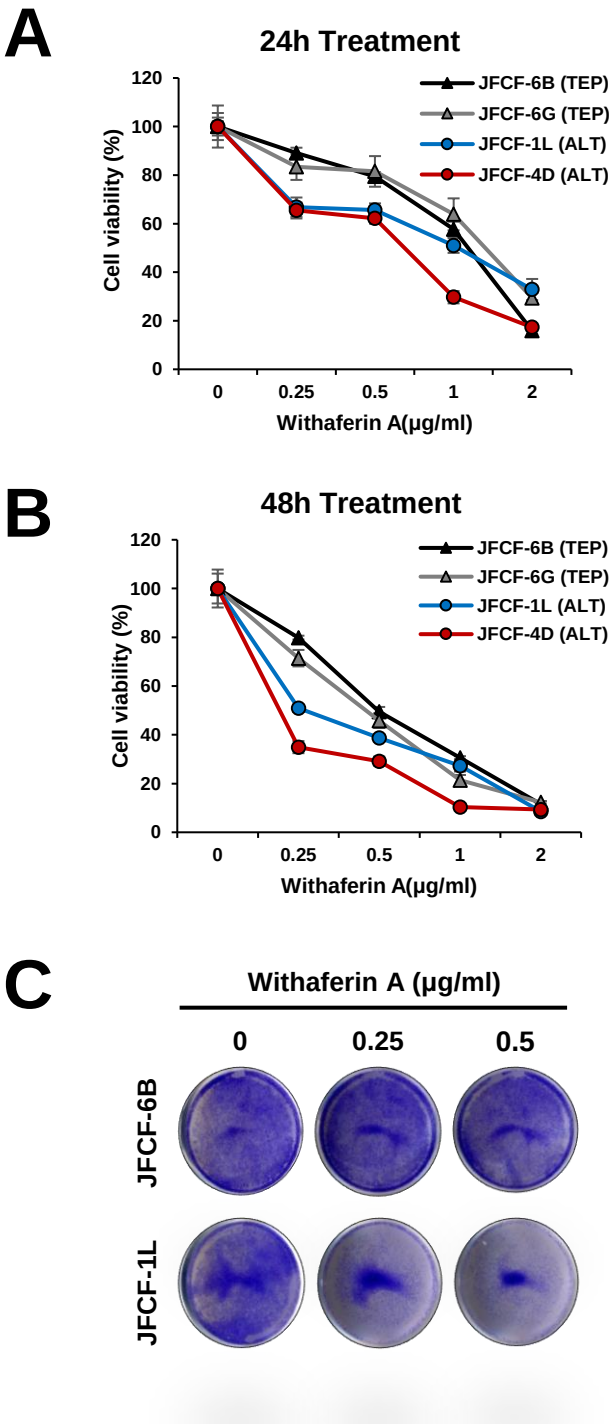

Fig. 2- 1 MTT assay (A and B) and Crystal violet staining (B) showed Withafein A exhibit stronger cytotoxicity to ALT cells, comparing to TEP cells.

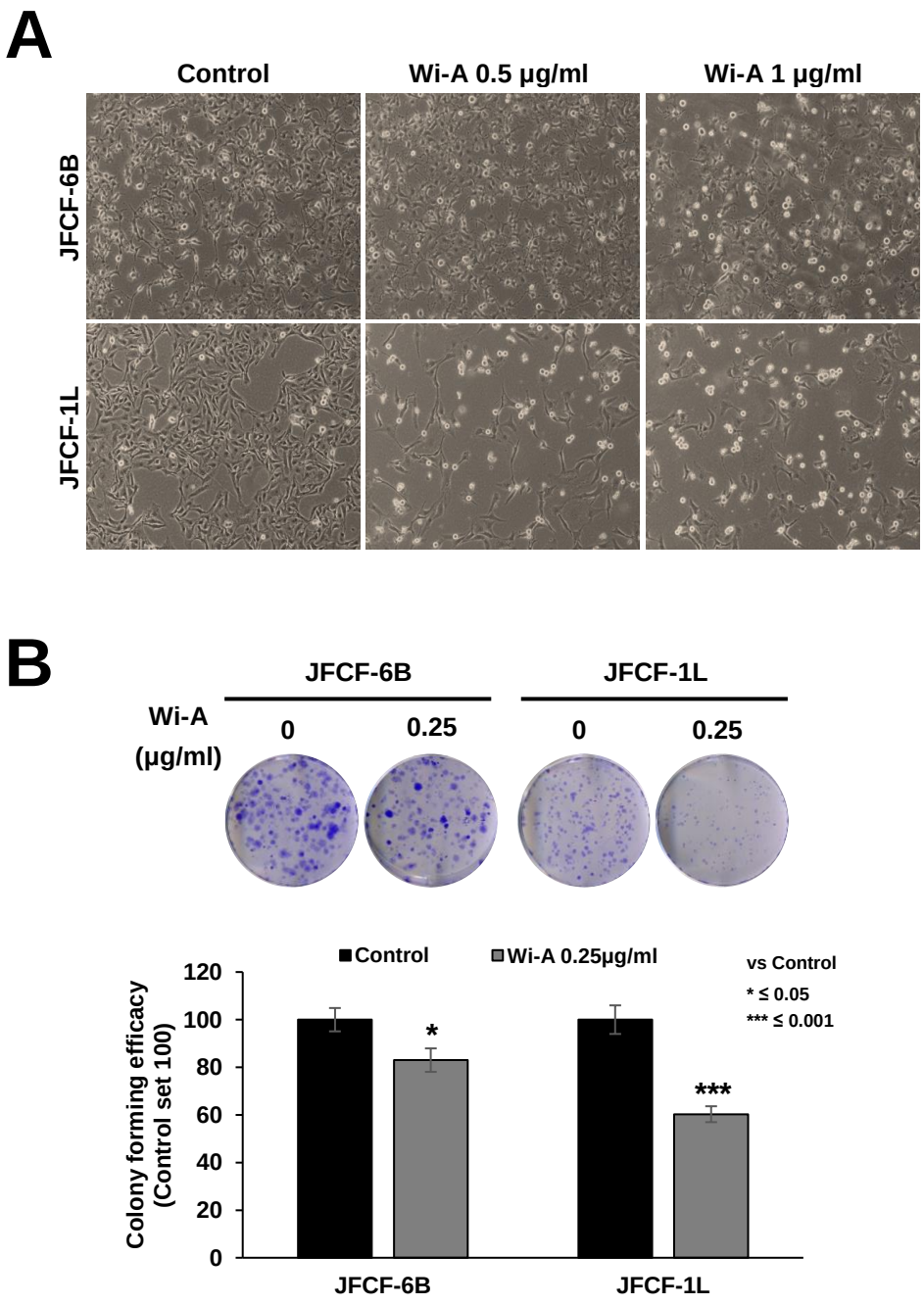

Fig. 2- 2 Effect of Withaferin A on the morphological changes (A) in JFCF-6B (TEP) and JFCF-1L (ALT) cells. Withaferin A show cytotoxicity to JFCF-1L even in low dose. Long-term colony forming assay (B) showed Wi-A treatment result in about 20% and 40% reduction in JFCF-6B and JFCF-1L cells, respectively.

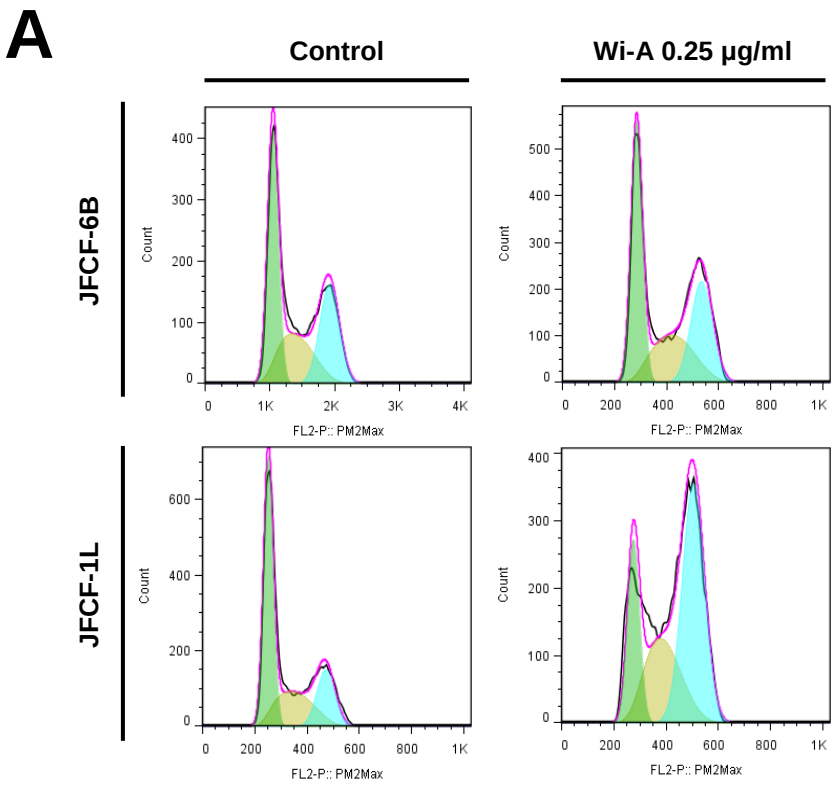

B

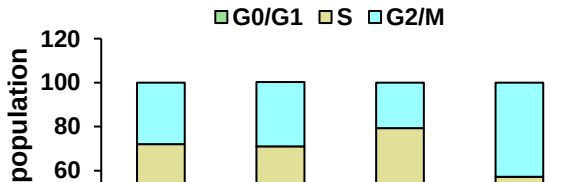

	JFCF-6B		JFCF-1L	
G2/M	28.0 ± 1.6	30.3 ± 1.6	20.6 ± 1.0	42.8 ± 1.9
S	19.3 ± 0.7	28.2 ± 2.1	26.9 ± 1.1	30.1 ± 1.4
G0/G1	52.7 ± 2.7	41.7 ± 1.8	52.4 ± 2.6	27.1 ± 1.5

Fig. 2- 3 Cell cycle analysis (A) of control and Withafein A treated cells is shown. Withafein A led to significant G2/M arrest in JFCF-1L but not in JFCF-6B. Quantitation of cell cycle distribution data (B) obtained from three independent experiments.

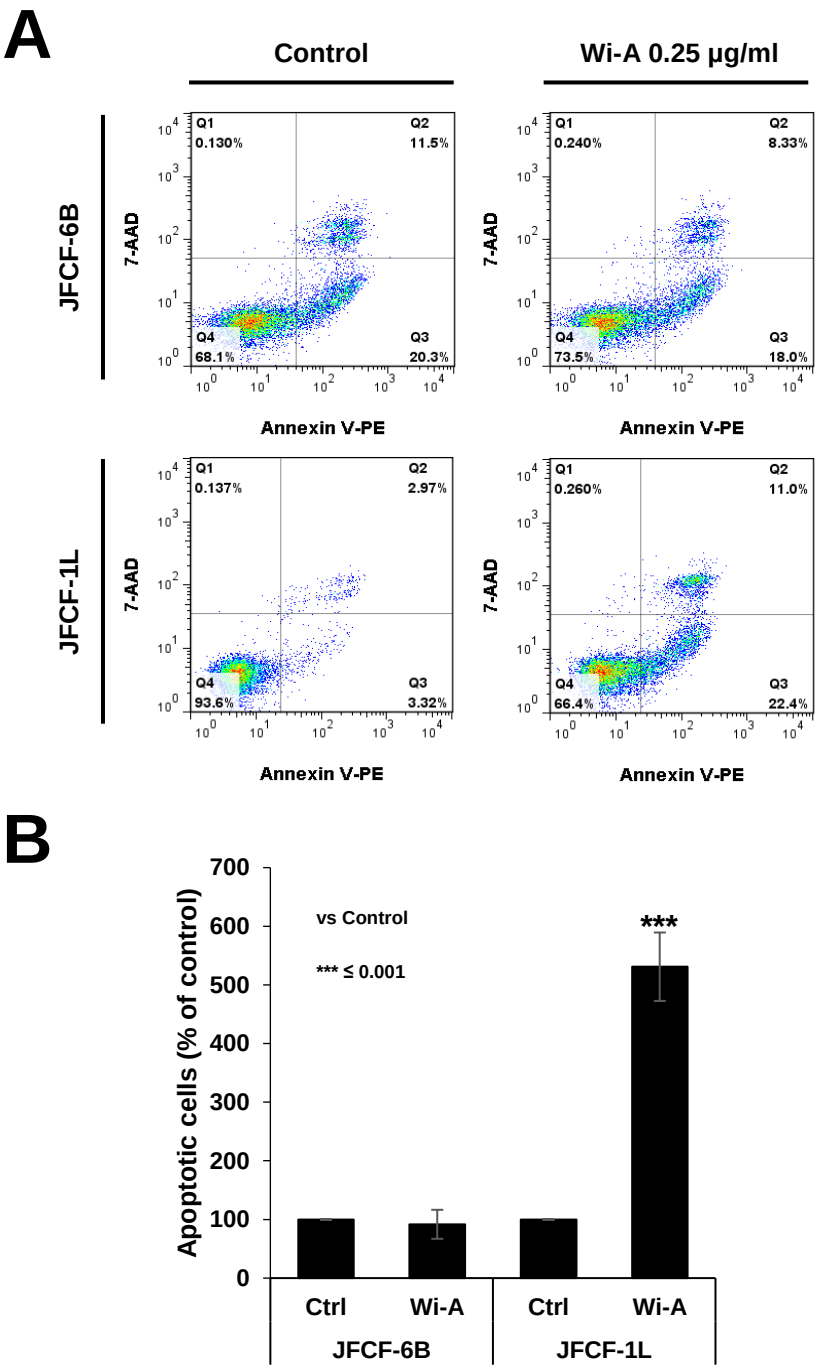

Fig. 2- 4 Withaferin A induced apoptosis in JFCF-1L(ALT) cell. Cells were treated with Withaferin A (0.25 μg/ml) for 24h, and apoptosis was analyzed by staining phosphatidylserine translocation with Annexin V/7-ADD. Annexin V positive (early and late apoptosis) cells were considered as the apoptotic population (A). Quantitation of apoptotic cells from three independent experiments is shown in B.

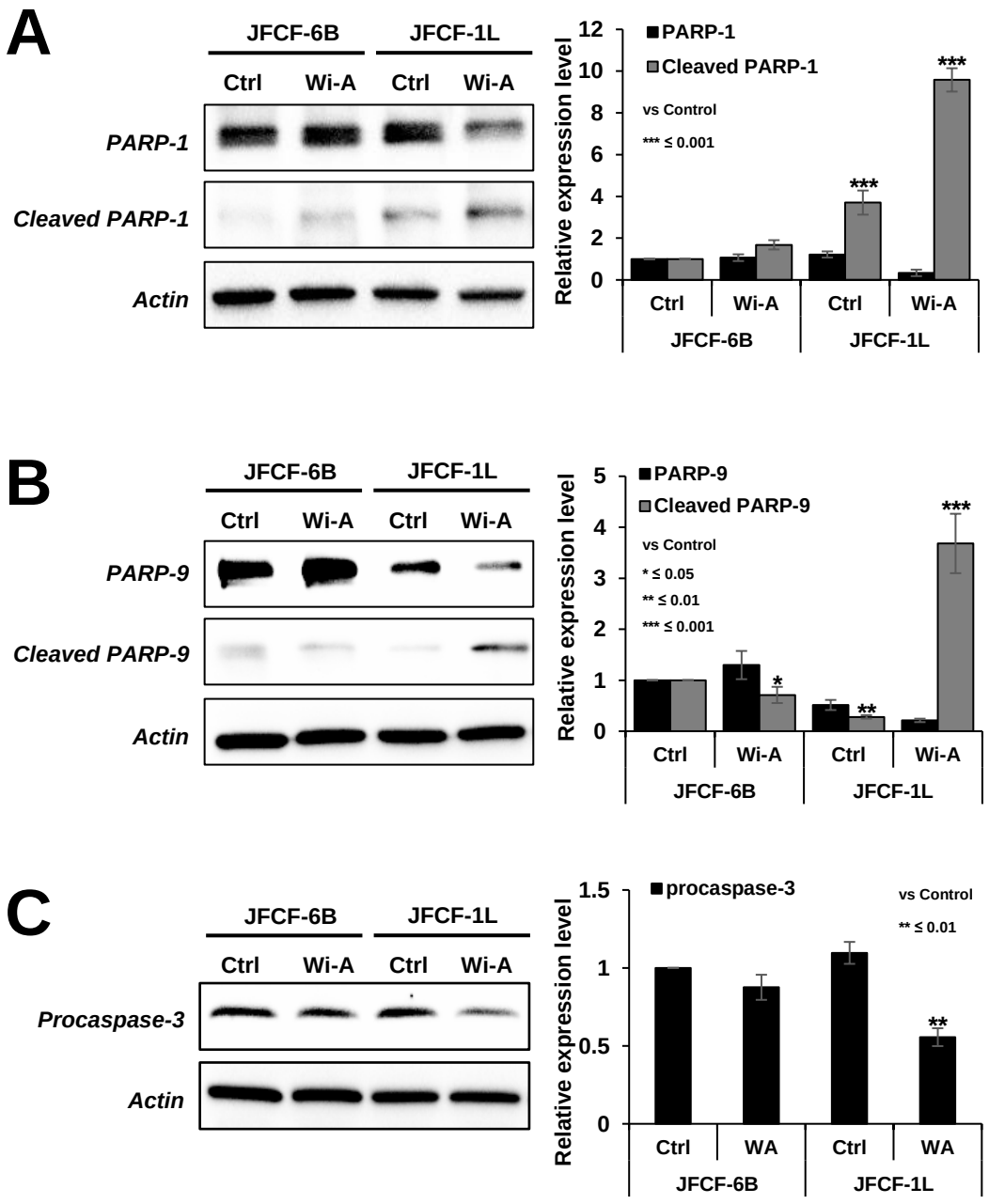

Fig. 2- 5 Western blotting analysis of apoptosis-associated proteins. An increase in cleaved PARP-1/9 (A and B) and decrease in procaspase-3 (C) were observed in JFCF-1L (ALT) cells in response to Withaferin A treatment. Quantitation results were represented as mean ± SD of three independent experiments.

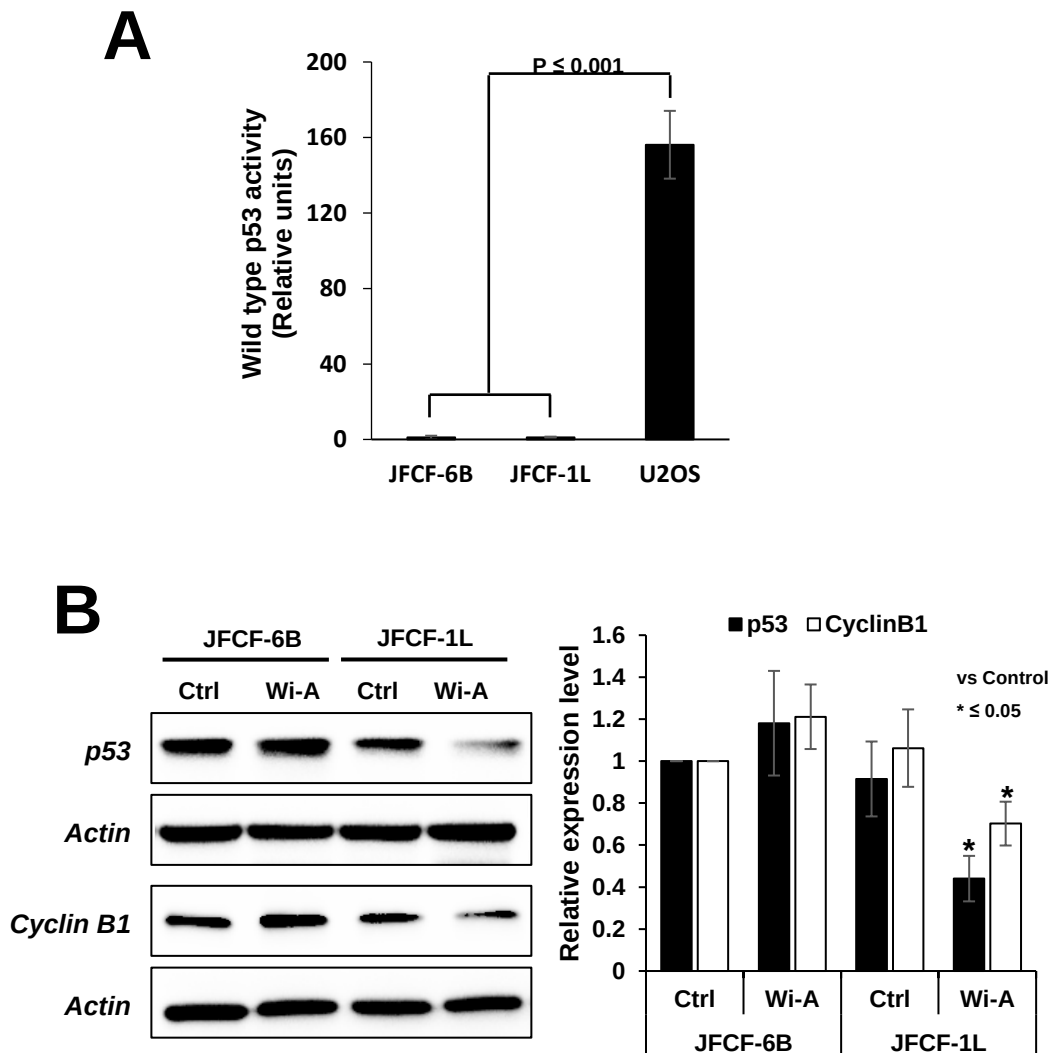

Fig. 2- 6 p53 promoter reporter assay showed JFCF series cells possess mutant type p53. U2OS served as positive control (A). p53 and cyclin B1 were evaluated by Western blotting in Withaferin A-treated JFCF cells with densitometric quantitation of representative blots from at least three independent experiments (B).

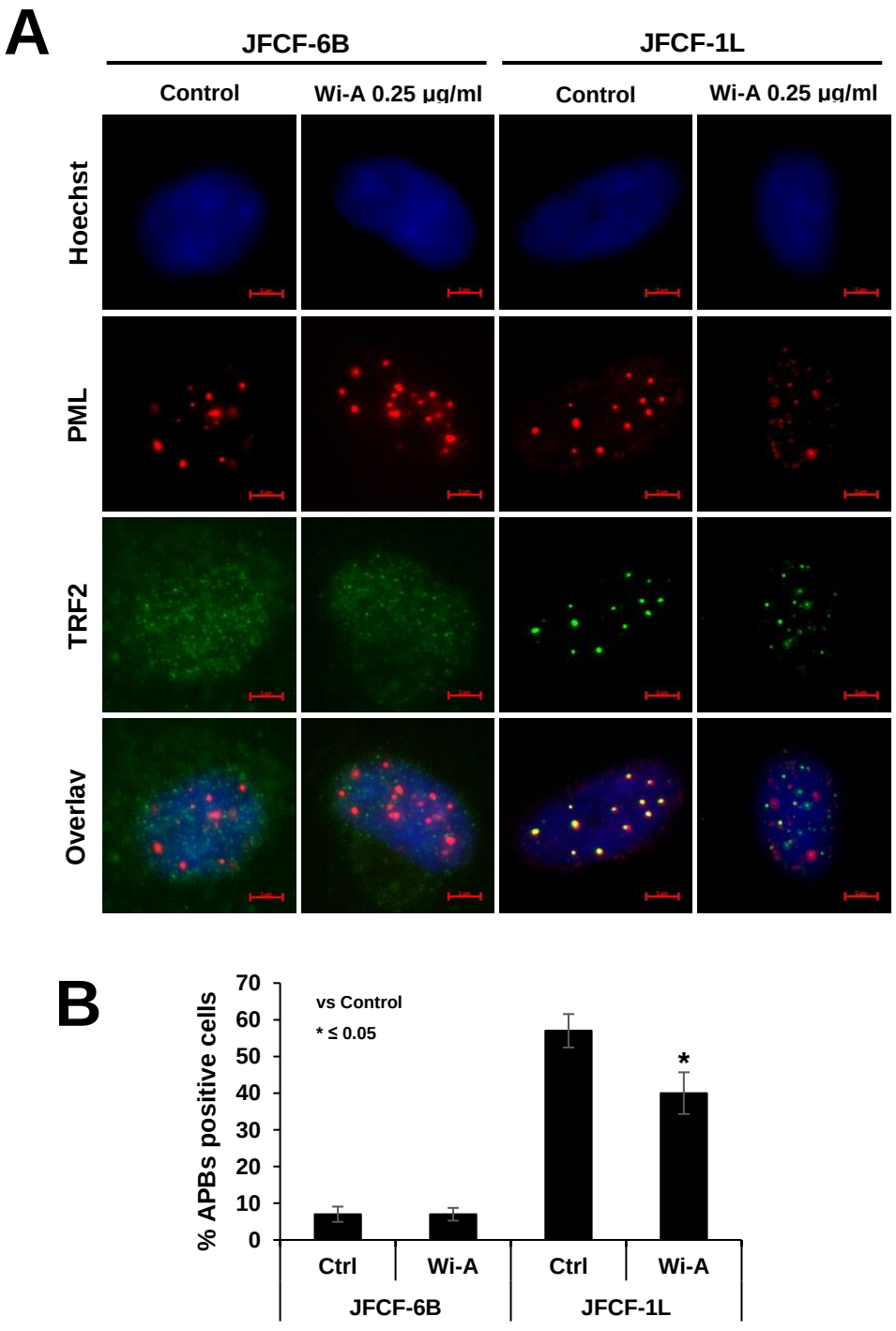

Fig. 2- 7 Double immunostaining of PML and TRF2 (A) showed a decreased number of APBs in JFCF-1L(ATL) cells after Withaferin A treatment. The number of APBs per cell was measured by colocalization of PML and TRF2 signals. 200 Cells with at least 3 signals were counted. Quantitation results were represented as mean ± SD of three independent experiments. Scale bar = 5 μm.

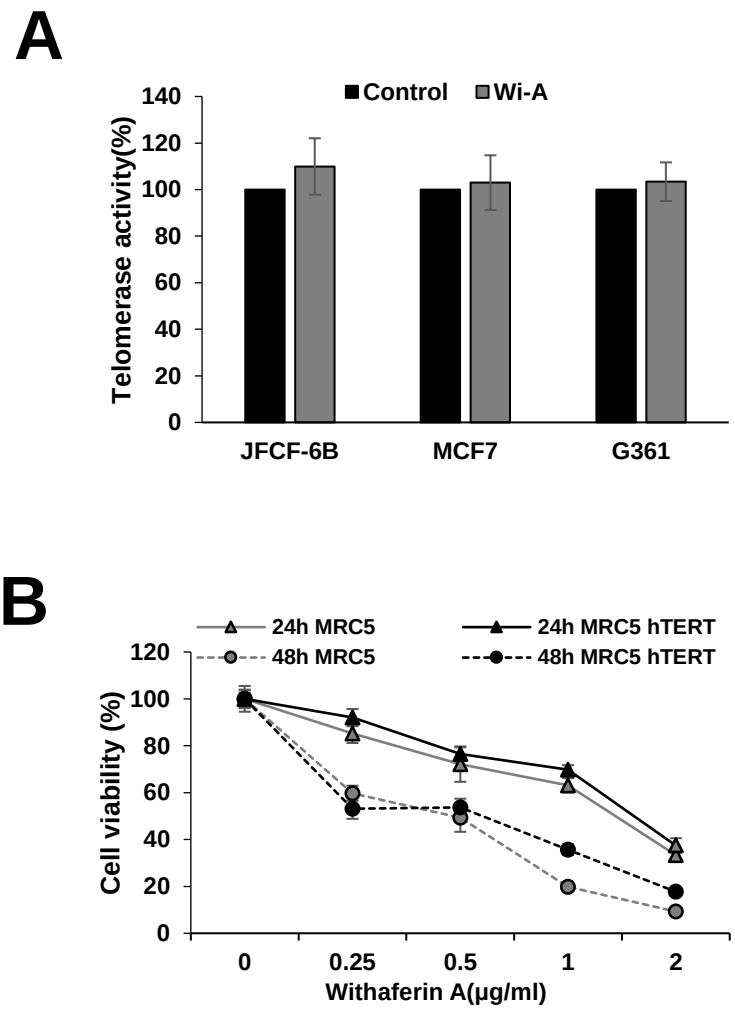

Fig. 2- 8 Effect of Withaferin A on telomerase activity. A series of telomerase positive cells (JFCF-6B, MCF7 and G361) were treated with Withaferin A, followed by TRAP assay analysis (A). Results of control and treated group were not statistically significant. ($p > 0.05$). Viability of MRC5 control and hTERT overexpressing cells was tested by MTT assay (B). Cells were incubated with Withaferin A for the 24 and 48h. Values were representative of three independent experiments and expressed as means.

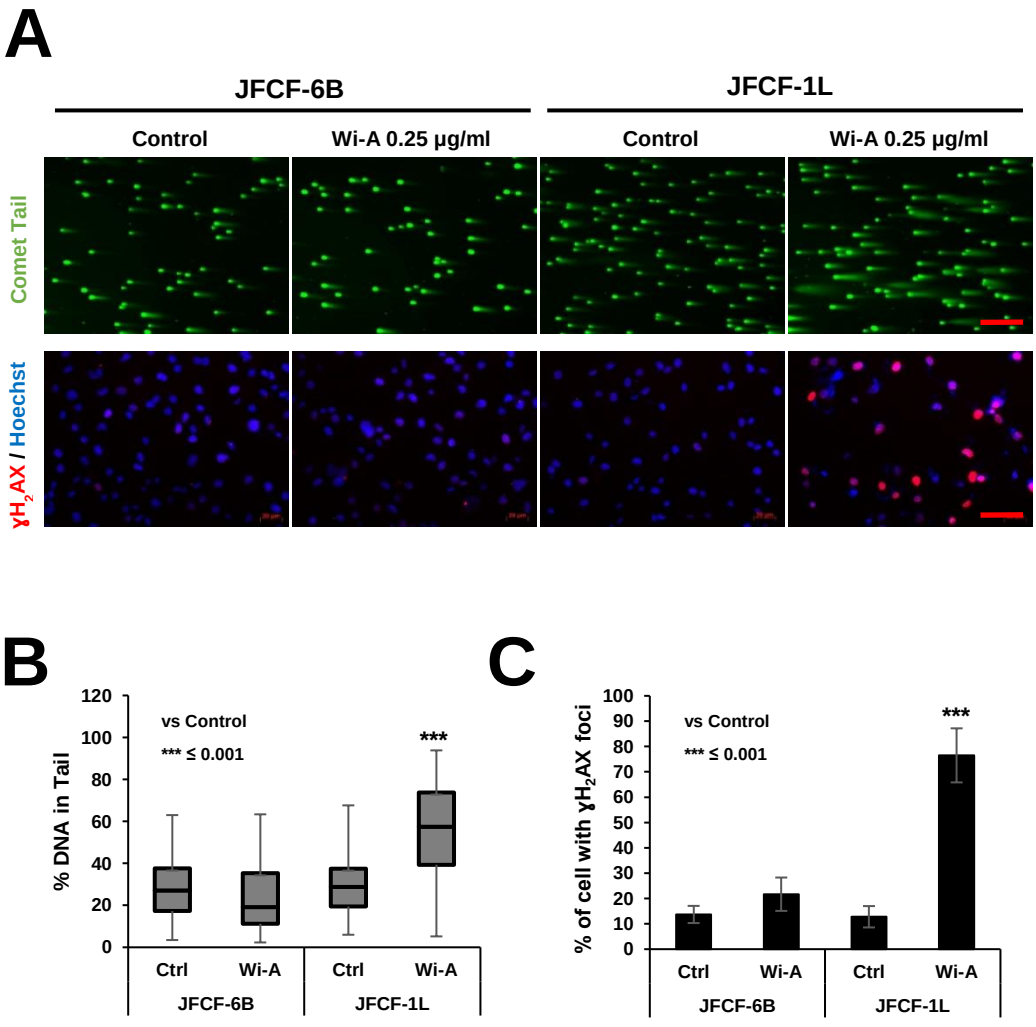

Fig. 2- 9 DNA damage induction in Withafein A treated JFCF-1L cells. Cells were treated with 0.25 µg/ml of Withaferin A for 24h , then subjected to Comet assay and immunostaining of DNA damage marker protein ɣH2AX (A). Percent of DNA in tail and ɣH2AX positive cells were quantified as shown in B and C, respectively. Scale bar = 40 µm.

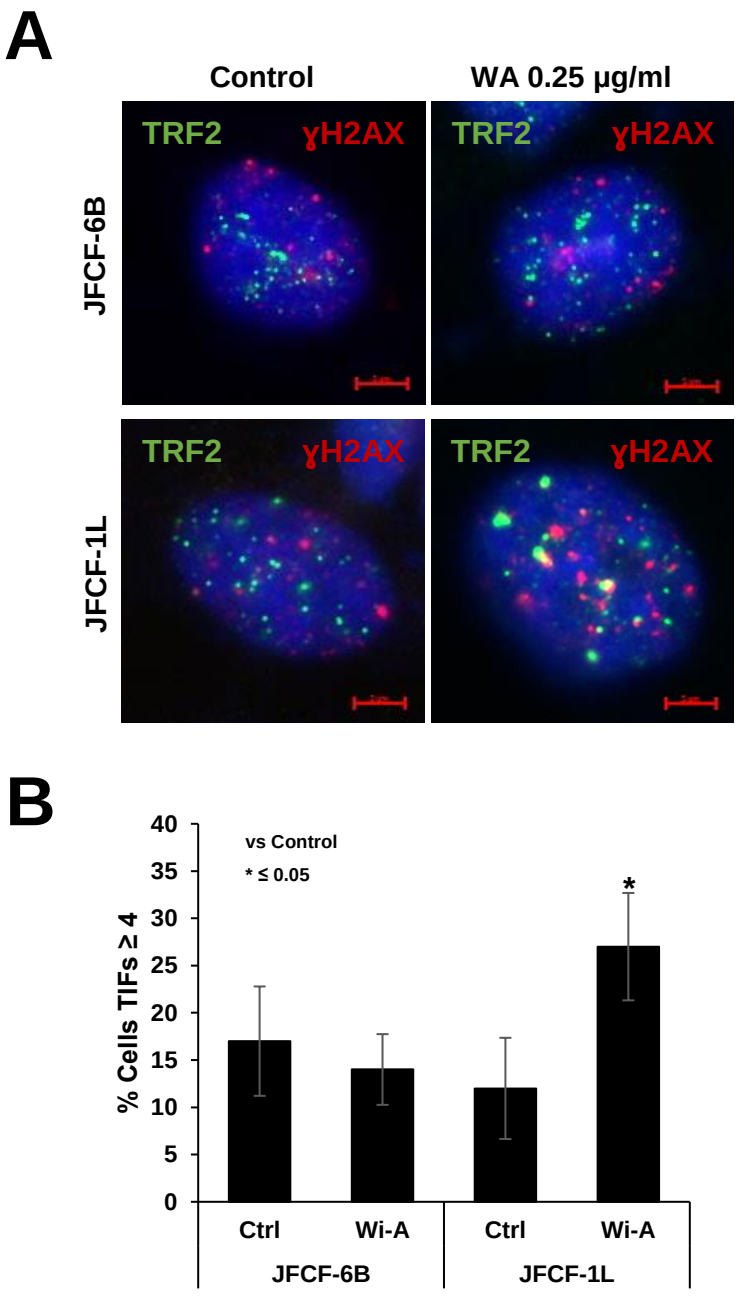

Fig. 2- 10 Withaferin A induced telomere dysfunction in JFCF-1L cell. Telomere dysfunction-induced foci (TIF) was measured by double immunostaining of TRF2 and γH2AX (A). Dysfunctional telomeres were recognized by Co-localization signals. Cells with at least 4 TIFs were counted as shown in B. Quantitation results were represented as mean ± SD of three independent experiments. Scale bar = 5 μm.

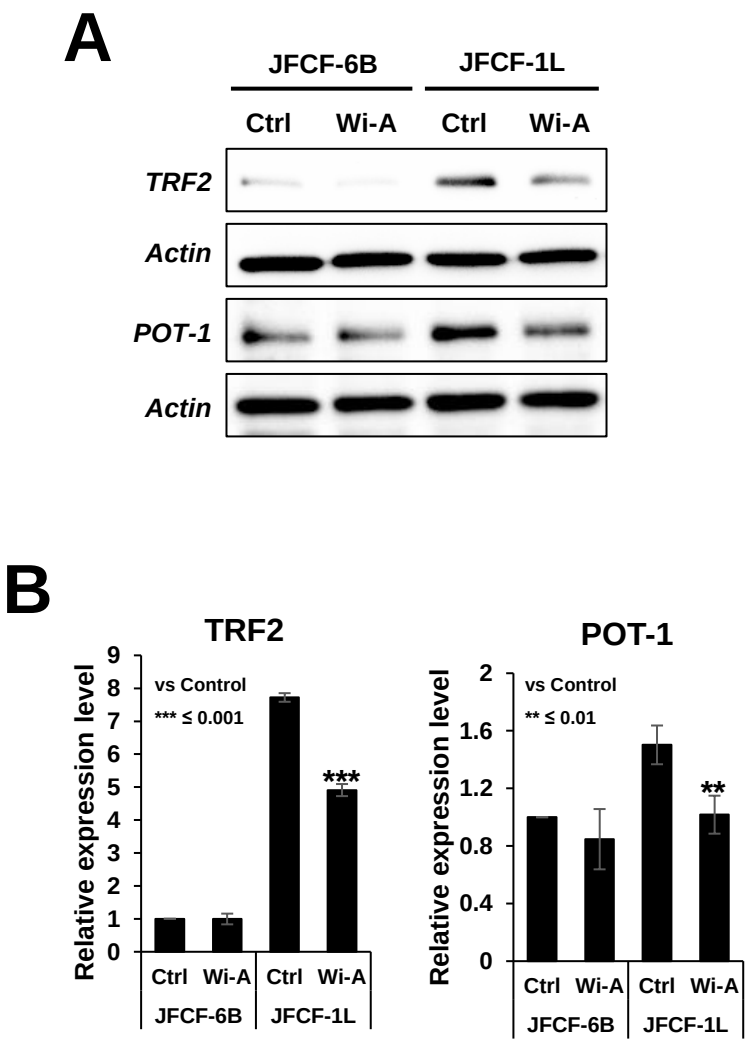

Fig. 2- 11 Western blotting analysis of telomere protection proteins. A decrease expression of TFR2 and POT1 was observed in JFF-1L(ALT) cells response to Withaferin A treatment (A). Quantitation results (B) were represented as mean ± SD of three independent experiments.

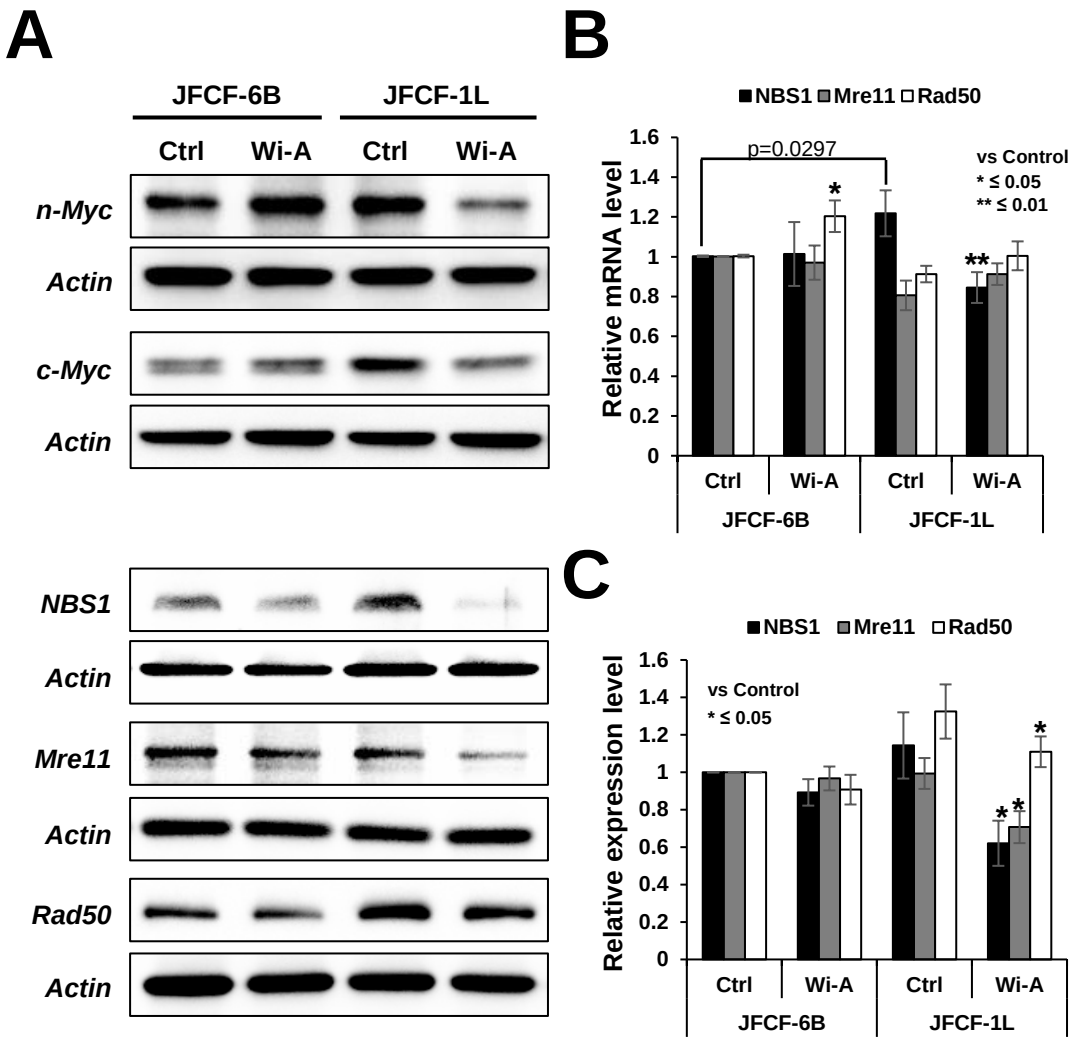

Fig. 2- 12 Western blotting of myc proteins (A) showed decrease level of expressin in JFCF-1L(ALT) cell in response of Withaferin A. MRN complex component proteins, myc downstream factors, were hence down-regulation by Withaferin-A in both mRNA (B) and protein (A and C) levels in JFCF-1L cell. Densitometric quantitation of representative blots are from at least three independent experiments (C).

Chapter 3 Noncoding regulation of drug induced DNA damage signaling and cellular senescence in ALT cells

3.1 Introduction

MicroRNAs (miRs) are a class of highly conserved small non-coding molecules (about 21-25 nucleotides long) that act as gene repressors by either causing their mRNA degradation or translational block. They are transcribed as pri-miRNAs and are subsequently processed into short hairpin structured molecules by Drosha, the double-stranded RNA specific ribonuclease. Their involvement in diverse biological processes ranging from normal development to a variety of pathogenesis has been implicated. Hence, miR profiling has been considered to yield valuable outcomes not only in the understanding of regulation of basic biological phenomena, but also in disease, diagnosis, therapy and prognosis [140-142].

Cancer is a complex disease. It is regulated by multifaceted network of signaling pathways driven by loss of activities of tumor suppressor proteins, gain of function of oncogenes and several epigenetic mechanisms [143-145]. Many miRs, including miR-21, miR-143, miR-145, miR-182 have been found as enriched in tumors and shown to possess oncogenic functions [146-148]. On the other hand, several others including miRNA-125b, miR-335-5p, and miR-34 family are down-regulated in several types of cancers [149-153]. Recently, it was shown that tumor suppressor protein p53 regulates miRNA expression and processing, and in turn is regulated by miRs. Restoration of p53-induced miRs was shown to cause suppression of tumor growth and metastasis in mouse models of cancer suggesting that there is a complex network of miR-p53 interactions in the regulation of p53 activities, its effectors and regulators [154-156]. Several other tumor suppressor pathways including pRB, PTEN, $p16^{INK4A}$, BMI and $p14^{ARF}$ have been shown to be either regulated by miRs or involve them for their activities to implement control on cell proliferation [157-161]. In spite of imperative emerging evidence of the role of several miRs in cancer, the molecular targets and

mechanisms remain largely undefined. In addition, a number of miRs have also been characterized to possess both tumor suppressor and oncogenic functions [162] warranting molecular insights to their activities in context of cell physiology.

Epigenetic control of cancer has been well established [145]. Several epigenetic drugs (DNA methyl-transferase and histone deacetylase inhibitors) that induce senescence in cancer cells have been in practice in conventional chemotherapy. However, their impact on the miRs and cancer progression remains largely unknown [163]. It was reported that miR-34 and miR-145 were silenced through DNA hypermethylation and were, hence, induced by 5Aza-dC treatment [164, 165]. In the present study, we used a bicistronic vector containing GFP reporter to arbitrarily induce miRs in human osteosarcoma (U2OS). Genomic integration of this vector was expected to induce transcription of sequences downstream to its integration sites. Based on the fact that more than 70% of the human genomic DNA constitutes protein-noncoding sequences, such random integration of the vector in genome was expected to induce a large variety of miRNAs (referred to as arbitrary miR library). Cells expressing such random library of miRs were subjected to 5-Aza-dC induced senescence for 3-5 days. Whereas untransduced controls showed senescence phenotype, some virus transduced cells escaped from 5-Aza-dC induced senescence (called loss of function) and was subjected to miR-array analysis with respect to the control (untransduced) cells. Out of several upregulated miRs, we aim to characterize the function of miR-335.

3.2 Materials and methods

3.2.1 Cell culture, transfections and drug treatments

Osteosarcoma (U2OS and Saos-2), cervical carcinoma (HeLa), breast adenocarcinoma (MCF 7 and MDA-MB-231), lung carcinoma (A549 and H1299) and normal human fibroblasts (TIG and WI38) were purchased from Japanese Collection of Research Bioresources (JCRB, Japan) and cultured in Dulbecco's modified Eagle's medium (DMEM; Gibco BRL, Grand Island, NY, USA) supplemented with 10% (v/v)

fetal bovine serum (Gibco BRL), and 1% (v/v) penicillin/streptomycin in the presence of 5% CO_2 at 37ºC. Transfection was performed using X-tremeGENE 9 DNA transfection reagent (Roche Applied Sciences, Basel, Switzerland). Transfected cells were selected using blasticidin (10 μg/ml). Cells were treated with 20 μM of 5-Aza-2'deoxycytidine (5-Aza-dC) (Sigma-Aldrich, St. Louis, MO, USA) for 48-96 h.

3.2.2 Induction of arbitrary miR library and screening for miRNAs involved in escape from 5Aza-dC induced senescence

To construct a retroviral vector pMXGbu, a short linker with 5'-gaattAGCGGAGGACAGTACTCCGATCGGAGGACAGTACTCCGTtcgac -3' was inserted between *EcoR*I and *Sal*I sites of pMXCRGb [166] by removing CMV-RFP cassette. Upon transduction, the upstream LTR of the vector drives GFP-Bsd fusion gene and the downstream LTR initiates random transcription. The transduced cells were selected in blasticidin (10 μg/ml) supplemented medium and were then subjected to 5-Aza-dC (20 μM) for 3-5 days. The cells were subsequently harvested to prepare total RNA (RNeasy Plus Mini Kit (QIAGEN).

3.2.3 Cloning of miR-335, expression plasmid

pCXGb-miR-335: a primary miR-335 region was amplified from human genomic DNA by PCR using the following primers: 5'-AACTCGAGTTCAGCCTTCATTGTTTAATCTTTACAACAGC-3' and 5'-AAGATATCTGTATGGACATGAAGCTTTTACTTCAACATTAG-3'. The PCR product was digested with *Sal*I and *Eco*RV and introduced into pCXGb as described earlier [167].

3.2.4 Senescence-associated β-galactosidase assay (SA-β-gal)

SA-β-gal detection kit (Senescence Cells Histochemical Staining Kit, Sigma-Aldrich) was used following manufacturer's instructions. Cells showing blue staining were considered positive and counted under the microscope. Quantitation from three

independent experiments was performed.

3.2.5 Flow cytometry

Control and transfected cells were harvested by trypsin (0.25%). Cell pellets were washed with cold PBS and then added drop-wise to pre-chilled 70% ethanol. The fixed cells were centrifuged at 800×*g* for 5 min at 4°C, washed with cold PBS twice and then re-suspended in 0.25 ml PBS. The cells suspensions were treated with RNase A at 37ºC for 1 h followed by brief centrifugation to discard supernatant. Cells were re-suspended in 200 µl of Cell Cycle Guava reagent (Millipore, Billerica, MA, USA), incubated for 30 min in dark, and analyzed by EasyCyte Guava cytometer (Millipore). The data were further analyzed using FlowJo software.

3.2.6 Cell viability, proliferation and colony forming assay

Equal number of control and transfected cells were plated in 96-well plates. After 48 h of incubation at 37°C, 100 µl of MTT (Sigma-Aldrich) in PBS (5 mg/ml) was added to each well. After 4 h of incubation at 37 °C, the supernatant was discarded and the precipitate was dissolved with 100 ml of dimethylsulfoxide (DMSO). Plates were then read on a microplate reader (infinite M200 PRO, TECAN) at 570 nm.

For cell proliferation assay, control and transfected cells were plated onto 12-well plates. Cells were harvested and counted in triplicates at the indicated time point using TC20^{TM}Automated Cell Counter (Bio-Rad, Hercules, CA, USA), with trypan blue exclusion to identify viable cells. Growth curves were generated for each cell line from three independent experiments.

For long-term cell viability and proliferation, colony-forming assay was performed. 500 cells were plated in a 6-well plate and left to form colonies for the next 10-15 days with a regular change of medium on every third day. Colonies were fixed with pre-chilled methanol/acetone (1/1, v/v) 10 min on ice, stained with 0.1% crystal violet solution, photographed and counted.

3.2.7 Cloning of pMIR-CARF-3'UTR plasmid

CARF-3'untranslated region (UTR) was amplified by PCR (initial 10 min denaturation step at 98ºC followed by 30 cycles of 98ºC for 30s, 55ºC for 30s and 72ºC for 30s, with a final annealing step at 72ºC for 10 min) using human genomic DNA with primers: 5'-GTTTAAACGTTTAAACTGTGTCCAAAATATCACTGC-3' and 5'-ACTAGTACTAGTCTAACAGACACGTTCAAC-3'. The PCR product was digested with *Pme*1 and *Spe*1, and then introduced into pMIR-REPORT™ Luciferase plasmid (Applied Biosystems, Forster, CA, USA) between these two sites.

3.2.8 Luciferase reporter assay

The pGL4-p53-3'UTR and pGL4-p21-3'UTR were generously provided by Dr. Chae-Ok Yun (Hanyang University, Seoul, South Korea). U2OS control and miR-335 transfected cells were transfected with 1 μg of luciferase constructs (pGL4-p53-3'UTR, pGL4-p21-3'UTR or pMIR-CARF-3'UTR), 100 ng of control vector oligonucleotide (pRL-TK or pMIR-REPORT™ β-gal control plasmid) using Lipofectamine 2000 (Invitrogen, Carlsbad, CA, USA). After 24 - 48 h, luciferase activity was measured using a dual luciferase reporter assay system and β-gal enzyme system (Promega, Madison, WI, USA) following the manufacturer's protocol. Experiments were carried out in triplicate and repeated at least three times.

3.2.9 RNA extraction and real-time qRT–PCR

Total RNA was isolated from cells using the RNeasy mini kit (Qiagen, Standford Valencia, CA, USA). The concentration and purity of RNA were determined by ultraviolet spectrophotometry (A260/A280 >1.9) using NanoDrop ND-1000 (Nanodrop Technologies, Wilmington, DE, USA).

For CARF mRNA expression analyses, equal amount of RNA were used for reverse transcription following the protocol of QuantiTect Reverse Transcription Kit (Qiagen). The real-time qRT-PCR (50ºC for 2 min; 95ºC for 10 min, 40 cycles of 95ºC for 15 s, 60ºC for 1 min; and 72 ºC for 30 s) was performed using SYBR® Select Master

Mix (Applied Biosystems in triplicate on the Eco™ real time system (Illumina, San Diego, CA USA). The real-time qRT-PCR results were analyzed and expressed as relative expression of threshold cycle value, which was then converted to x-fold changes ($2^{-\Delta\Delta Ct}$) following manufacturer's instructions. The primer sets included: $p16^{INK4a}$ (1), 5'-CCCAACGCACCGAATAGTTA-3' (forward) and 5'-ACCAGCGTGTCCAGGAAG-3' (reverse); $p16^{INK4a}$ (2), 5'-GAAGGTCCCTCAGACATCCCC -3' (forward) and 5'-CCCTGTAGGACCTTCGGTGAC -3' (reverse); $p16^{INK4a}$ (3), 5'-CCCCTTGCCTGGAAAGATAC -3' (forward) and 5'-AGCCCCTCCTCTTTCTTCCT -3' (reverse); Rb, 5'-GGAAGCAACCCTCCTAAACC -3' (forward) and 5'-TTTCTGCTTTTGCATTCGTG -3' (reverse); CARF, 5'-TCAAAGTGACAGATGCTCCA -3' (forward) and 5'-CGTTGAACTGTTTTCCTGCT -3' (reverse); 18s, 5'-CAGGGTTCGATTCCGTAGAG -3' (forward) and 5'-CCTCCAGTGGATCCTCGTTA -3' (reverse).

For miR-335 expression analysis, the corresponding miR-335 (Assay ID: 000546) and RNU6B (Assay ID: 001093) primers and TaqMan® MicroRNA assay was performed following the manufacturer's instructions (Applied Biosystems). RNU6B served as an endogenous control for normalization. Real-time qRT-PCR reaction was conducted at 95°C for 10 min, followed by 40 cycles of 95°C for 15 s and 65°C for 1 min.

3.2.10 Western blotting

Cells were harvested using RIPA buffer (Thermo Scientific, Waltham, MA, USA) supplemented with a protease inhibitor cocktail (Roche). The protein concentrations were determined by using the Pierce BCA Protein Assay Kit (Thermo Scientific). Western blotting was performed by using following antibodies: anti-p16 (C-20), anti-p21 (C-19), anti-p53 (DO-1), anti-MDM2 (HDM2-232), anti-Cdk4 (C-22), anti-E2F

(MH5), anti-GFP (B-2) (Santa Cruz, CA, USA), anti-Phospho-Rb (Ser780), anti-Rb (4H1) (Cell Signaling, Danvers, MA, USA) and anti-CARF (FLA-10)[168]. Anti-β-actin antibody (AC-15) (Abcam, Cambridge, MA, USA) was used as an internal loading control. All the experiments were performed in triplicate at least three times.

3.2.11 Immunostaining

Cells were cultured on a glass coverslip placed in a 12-well culture dish. For immunostaining, cells were washed (cold PBS), fixed (pre-chilled methanol/acetone (1:1) mixture for 10 min), permeabilized (0.5% Triton X-100 in PBS for 10 min), blocked (0.2% BSA/PBS for 1 h) and were then incubated with specific antibody (as described above) for overnight at 4°C. They were incubated with Alexa-594-conjugated goat anti-mouse or anti-rabbit (Molecular Probes, Invitrogen) secondary antibodies after washings (thrice) with 0.2% Triton X-100 in PBS. Counterstaining was performed with Hoechst 33342 (Sigma) for 10 min in dark following by extensive washings with 0.2% Triton X-100 in PBS and observations under a Carl Zeiss microscope (Axiovert 200 M, Tokyo, Japan) .

3.2.12 *In vivo* tumor formation assay

Balb/c nude mice (4 weeks old, female) were provided by the Institute of Laboratory Animal Science of Peking Union Medical College, China. Cells (A549 and A549-miR335 derivatives) were injected into the nude mice subcutaneously (5×10^6 suspended in 0.2 ml of growth medium). Tumor formation and mice health (body weight) was monitored every alternate day. The experiment was repeated twice, using 4 mice in each group. Volume of the subcutaneous tumors was calculated as $V=L \times W^2/2$, where L was length and W was the width of the tumor, respectively. Protocols for animal experiments were approved by the Animal Care and Use Committee, Institute of Laboratory Animal Science of Peking Union Medical College, China (ILAS-PG-2014-018).

3.2.13 miRNA array

Control (untransduced and untreated) and virus transduced and 5-Aza-dC (20 μM) treated cells (pooled colonies) that escaped senescence were harvested. For miRNA microarray, small RNAs (less than 200 nt including precursor and mature miRNAs) were extracted using mirVana miRNA isolation kit (Ambion, Austin, TX, USA) following the manufacturer's protocol. Purified RNA was labeled with Cy3 or Cy5 using the mirVana miRNA labeling kit (Ambion). Labeled RNA was hybridized with oligonucleotides against human miRs arrayed on slides (Hokkaido-System Science, Japan), and detected by a scanner (Agilent Technologies, Santa Clara, CA, USA).

3.2.14 Statistical analysis

All experiments were carried out in triplicates, and data were expressed as mean ± standard deviation (SD). Two-tailed Student's t-test or nonparametric ManneWhitney U-test, whichever was applicable, was used to determine the degree of significance between the control and experimental sample. Statistical significance was defined as p-value ≤ 0.05.

3.3 Results and discussion

3.3.1 Identification of miR-335 in loss-of-function screening of miRs involved in escape of 5-Aza-dC induced senescence

A retroviral vector constituting two long terminal repeat (LTR) promoters on the 5' and 3' ends of the gene for GFP was generated in a way that the random integration of this vector in the genome would result into (i) expression of GFP; detected by green fluorescence and (ii) its integration-dependent arbitrary manipulation of the host cell genome. The latter may yield loss of function phenotype due to altered expression of either proteins or their noncoding regulators miRs. We coupled this system with induction of senescence in human cancer cells (U2OS) by demethylating drug, 5-Aza-dC. The cells that escaped senescence were selected by their propagation and were

subjected to microRNA array with respect to the untreated control cells (Fig. 3-1). We found that several miRNAs (miR-101, miR-143, miR-145, miR-335, miR-451, miR-545 and miR-558) were upregulated in vector-transduced cells that showed resistance to 5-Aza-dC induced senescence (Fig. 3-1). Of note, two of these miRs (miR-145 and miR-335) have been reported to undergo hypermethylation-mediated silencing in a large variety of cancers [164, 169] and hence their upregulation by 5-Aza-dC induced demethylation was justified. Furthermore, our data suggested that these miRs are involved in regulation of induction of cellular senescence, proliferation and drug response of cells. We aimed to characterize such functions and targets of miR-335 in this study.

3.3.2 miR-335 compromises 5-Aza-dC induced senescence by retard of cell cycle progression

An expression plasmid encoding primary miR-335 was transfected into U2OS cells. Treatment of control or miR-335 derivatives with 5-Aza-dC and detection of senescent cells by senescence associated β-gal staining revealed that miR-335 compromised induction of senescence. There was about 50% reduction in the SA-β-gal positive cells in miR-335 derivatives (Fig. 3-2A). Cell viability analysis also showed resistance of miR-335 derivatives to 5-Aza-dC at all doses tested (Fig. 3-2B) suggesting that the upregulation of miR-335 was involved in the escape of cells from 5-Aza-dC induced senescence/growth arrest. We further examined if induction of senescence involved downregulation of miR-335 expression. 5-Aza-dC treated cells were collected and subjected to miR-335 expression analysis. We found that miR-335 was downregulated in these cells (Fig. 3-2C), endorsing the role of upregulated miR-335 in escape of cells from senescence. Taken together, these data suggested that miR-335 is downregulated in cells that showed senescence upon 5-Aza-dC treatment, and that overexpression of miR-335 suppressed the senescent phenotype.

In order to clarify the mechanism of this phenomenon, we considered two

possibilities: (i) Based on the fact that incorporation of 5-Aza-dC takes place during replication and DNA synthesis, we hypothesized that miR-335 might cause growth arrest of cells leading to the situation that 5-Aza-dC was not incorporated into the genome, and (ii) miR-335 may target genes that are essential for 5-Aza-dC induced growth arrest. We tested the possibility (i) by analyzing the growth and cell cycle characteristics in control and miR-335 derivatives. As shown in Figs. 3-3, the latter were retarded in their growth (A) and showed lower viability (B) in short term as well as long term colony-formation assays (C). Cell cycle analysis revealed increase in number of cells at G0/G1, G2/M and decrease in S phase (Fig. 3-4A). These data suggested that miR-335 caused growth arrest of cells that may have contributed, at least in part, to the escape of cells to 5-Aza-dC induced senescence as hypothesized above. Growth arrest function of miR-335 was also confirmed by *in vivo* subcutaneous xenografts of control and miR-335 derivatives of A549 cells in nude mice (Fig. 3-4B). We found that the tumor growth of miR-335 derivatives was suppressed as compared to the control cells. Physiological relevance of miR-335 was determined by its expression analysis in normal and cancer cells. Consistent with its role in growth arrest, miR-335 expression was high in normal fibroblasts as compared to a variety of cancer cells (Fig. 3-4C). Furthermore, consistent with induction of growth arrest and tumor suppressor activity of miR-335, the miR-335 overexpressing cells showed upregulation of $p21^{WAF1}$ and downregulation of CDK4 (Figs. 3-5A and 5B).

3.3.3 Effect of miR-335 on $p16^{INK4A}$ and pRB resulting in compromised 5-Aza-dC-induced senescence

We next considered the second possibility that the miR-335 may target essential genes involved in 5-Aza-dC induced growth arrest. In U2OS cells, $p16^{INK4A}$ (cyclin-dependent kinase inhibitor and tumor suppressor) is known to undergo silencing by hyper-methylation of its promoter [170]. As expected, 5-Aza-dC treated cells showed induction of $p16^{INK4A}$ (Figs. 3-6A and 6B). Of note, we found that miR-335 transfected

cells showed downregulation of 5-Aza-dC induced $p16^{INK4A}$ protein expression suggesting that miR-335 may target $p16^{INK4A}$ directly or indirectly and hence may account for escape of 5-Aza-dC induced senescence in miR-335 transfected cells. In order to confirm this, we determined the expression of $p16^{INK4A}$ in control and miRNA-transfected cells by qPCR using three sets of primers and, surprisingly, found increase in $p16^{INK4A}$ transcript in 5Aza-dC treated control as well as miR-335 overexpressing cells (Fig. 3-6C). These data suggested that decrease in $p16^{INK4A}$ protein observed in miR-335 overexpressing cells was not due to direct targeting of $p16^{INK4A}$ mRNA by miR-335.

$p16^{INK4A}$ is an established inhibitor of cyclin D-CDK4 complex. The latter phosphorylates retinoblastoma protein resulting in dissociation of pRB-E2F1 complex and cell cycle progression that requires free E2F1. Accordingly, targeting of $p16^{INK4A}$ by miR-335 was expected to result in activated cyclin D-CDK4 complex resulting in increased level of phosphorylated pRB in miR335 derivatives. We examined the levels of pRB and phospho-pRB and found, contrary to the expected, decrease in phospho-pRB in miR-335 derivatives (As shown in Fig. 3-7A). Western blotting with pRb and phospho-pRB specific antibodies also confirmed their downregulation in miR-335 derivatives (Fig. 3-7B). qPCR analysis also revealed decrease in pRB transcript in miR-335 overexpressing cells (Fig. 3-7C), endorsing that miR-335 targets pRB. In light of this data, decrease in phosphorylated-pRB was accounted for cell cycle retardation, and hence escape of cells from 5-Aza-dC induced senescence. Another study also showed that during differentiation of mouse embryonic stem cells, miR-335 is upregulated and causes down regulation of Oct4-pRB axis and pRB dephosphorylation [158]. In this report, miR-335 was shown to target pRB directly and specifically targeting a conserved sequence motif in its 3' un-translated region [157]. However, it was shown to result in consequential activation of p53 tumor suppressor resulting in inhibition of cell proliferation and transformation. Taken together with our findings, it emerged that miR-335 is an important miR that controls cell proliferation by balancing the activities of

the pRB and p53 tumor suppressor pathways.

3.3.4 miR-335 targets CARF and compromises 5-Aza-dC induced senescence

In light of the information that miR-335 targets pRB and activates p53 [157], we examined the level of p53 in control and miR-335 derivatives. As shown in Fig. 4, we found decrease in p53 protein level in miR-335 derivatives (Figs. 3-8A and 8B, Fig. 3-9A). We next determined the mechanism of such decrease and its impact in escape of cells from 5-Aza-dC induced senescence. Since p53 is degraded by its antagonist HDM2, we examined its level of expression in control and miR-335 derivatives. As shown in Figs. 3-8 and 3-9, miR-335 derivatives showed higher level of HDM2 by Western blotting (Figs. 3-8A and 8C) as well as immunostaining (Fig. 3-9B) suggesting that miR-335 may target an upstream inhibitor of HDM2, leading to its increased levels that in turn caused decrease of p53 in miR-335 derivatives.

CARF (Collaborator of ARF), a protein that poses two-way control on cell proliferation, has been shown to be an upstream regulator of p53 [171-173]. Whereas its upregulation occurred during replicative and premature senescence, its super-high level was shown to be associated with tumorigenesis and malignant transformation of cancer cells[174]. It was shown to act as a transcriptional repressor of HDM2 (an antagonist of p53) [175]. In view of above findings on miR-335, we examined CARF-p53-HDM2-p21 axis in miR-335 cells. As shown in Fig. 3-10, these cells showed down-regulation of CARF at protein (A and C) as well as mRNA (B) levels implying that miR-335 targets CARF, and may account for increased level of HDM2 and decreased level of p53 (Figs. 3-8 and 3-9).

In order to finally resolve whether miR-335 directly targets CARF, p53 and $p21^{WAF1}$, we performed reporter assays using 3'UTR regions of these genes. As shown in Fig. 3-11A, we found that CARF, but not p53 and $p21^{WAF1}$, was the target of miR-335. As shown in Figs. 3-5A and 5B, contrary to the decreased level of expression of p53, its downstream effector and major regulator of growth arrest, $p21^{WAF1}$ showed increase in miR-335 derivative cells. This was in line with our recent findings that high

level of CARF expression acts as a repressor of $p21^{WAF1}$ [176] and hence targeting of CARF by miR-335 accounted for increase in $p21^{WAF1}$ and growth arrest of miR-335 derivatives in spite of knockdown of $p16^{INK4A}$ and pRB (Fig. 3-6 and 3-7). $p21^{WAF1}$-promoter luciferase reporter assays in control and miR-335 derivatives also showed increase in $p21^{WAF1}$ reporter activity in miR-335 overexpressing derivatives (Fig. 3-11C). Furthermore, we determined that this increase in $p21^{WAF1}$ was independent to that of p53 by using p53-/- cells (Saos-2). As shown in Fig. 3-11B, miR-335 derivatives showed decrease in CARF and increase in $p21^{WAF1}$ suggesting that miR-335 targets CARF and caused increase in $p21^{WAF1}$ independent to that of p53. In order to resolve if miR-335 is involved in senescence induced by other drugs, we subjected cells to retinoic acid- and doxorubicin-induced senescence. As shown, CARF increased and miR-335 decreased in drug-treated cells that caused growth arrest (Fig. 3-11D).

CARF is an essential cell proliferation-regulatory protein that is upregulated during replicative and stress-induced senescence. Suppression of CARF induced aneuploidy, DNA damage and mitotic catastrophe resulting in apoptosis endorsing that it is an essential for cell survival [172]. It has been shown to bind to multiple proteins, $p14^{ARF}$, p53 and HDM2 of ARF-p53-p21 tumor suppressor axis and control cancer cell proliferation in two directions in a dose dependent way [171, 174, 177]. It was shown that while moderate level of CARF overexpression induced senescence, its very high level resulted in increased cell proliferation. Hence, CARF was demonstrated to determine the proliferative fate of cancer cells towards growth arrest or pro-proliferative and malignant phenotypes by feedback and feed-forward regulatory loops of CARF-ARF-p53-HDM2-$p21^{WAF1}$ axis. Molecular mechanism(s) of such dual regulation and how CARF is regulated in normal and cancer cells have not been fully understood. It was shown that CARF is involved in drug-induced senescence [171] and hence its knockdown by miR-335, induced by 5-Aza-dC mediated demethylation accounts, at least in part, for escape of cells from 5-Aza-dC induced senescence.

3.3.5 Wi-A causes induction of miR-335, resulting in down-regulation of CARF in TEP cells

In light of the mechnism we presented in Fig. 3-12B, miR-335 caused cell cycle retard through regulation of CARF. In Chapter 2, results showed that Wi-A treatment led to cell growth suppression, and finally induced apoptosis. Such similar phenotype drove us to suspect whether miR-335 was involved in Wi-A-mediated physiological activities. Hence, we conducted qPCR analysis and found miR-335 was only up-regulated by Wi-A treatment in JFCF-6B TEP cell (Fig. 3-13A). We examined the expression level of CARF. As we expected, Wi-A treatment decreased CARF expression in TEP cells, while Wi-A treated ALT cells showed no difference with respect to the control group (Fig. 3-13B). Western blotting for p21 and CDK6 revealed up-regulation of p21 and down-regulation of CDK6 in TEP cells by Wi-A treatment, whereas variation trend in ALT cells was relatively moderate (Fig. 3-13B). Of note, we found the CARF expression level in ALT cells was less than TEP cells. Such a lower expression of CARF might make ALT cells insensitive to miR-335-mediated growth suppression. Considering the fact that ALT cells showed more DNA damage than TEP cells during Wi-A treatment (Fig. 2-10 and 2-9), it may be possible Wi-A-induced growth retardation gains the repairing time of DNA damage for JFCF-6B TEP cells, which blunts the induction of apoptosis as shown in Chapter 2.

3.4 Summary

We demonstrated that CARF is a new target of miR-335 that mediates its tumor suppressor function. Pleotropic effects of miR-335 demonstrated in the present study and others (as discussed above) may be due to, at least in part, its control on CARF expression that has been shown to impose a dose dependent and contrasting effect on proliferation and malignant transformation of cancer cells. We demonstrated that targeting of CARF by miR-335 resulted in upregulation of $p21^{WAF1}$, downregulation of cyclin-CDK activity (Fig. 3-5). Furthermore, CARF has also been shown to cause

upregulation of $p16^{INK4A}$ [31]. Hence CARF-targeting by miR-335 also accounted for downregulation of $p16^{INK4A}$ protein (Fig. 3-6A and 6B) in spite of the fact that $p16^{INK4A}$ mRNA was increased in miR-335 and 5-Aza-dC treated cells. These data suggested miR-335 effects (such as, decrease in $p16^{INK4A}$ protein, increase in HDM2 and $p21^{WAF1}$) and outcomes such as growth arrest are determined predominantly by CARF-targeting.

Taken together, CARF emerged as a new strong target of miR-335, demanding further studies for its potential as an important noncoding tumor suppressor in cancer therapeutics.

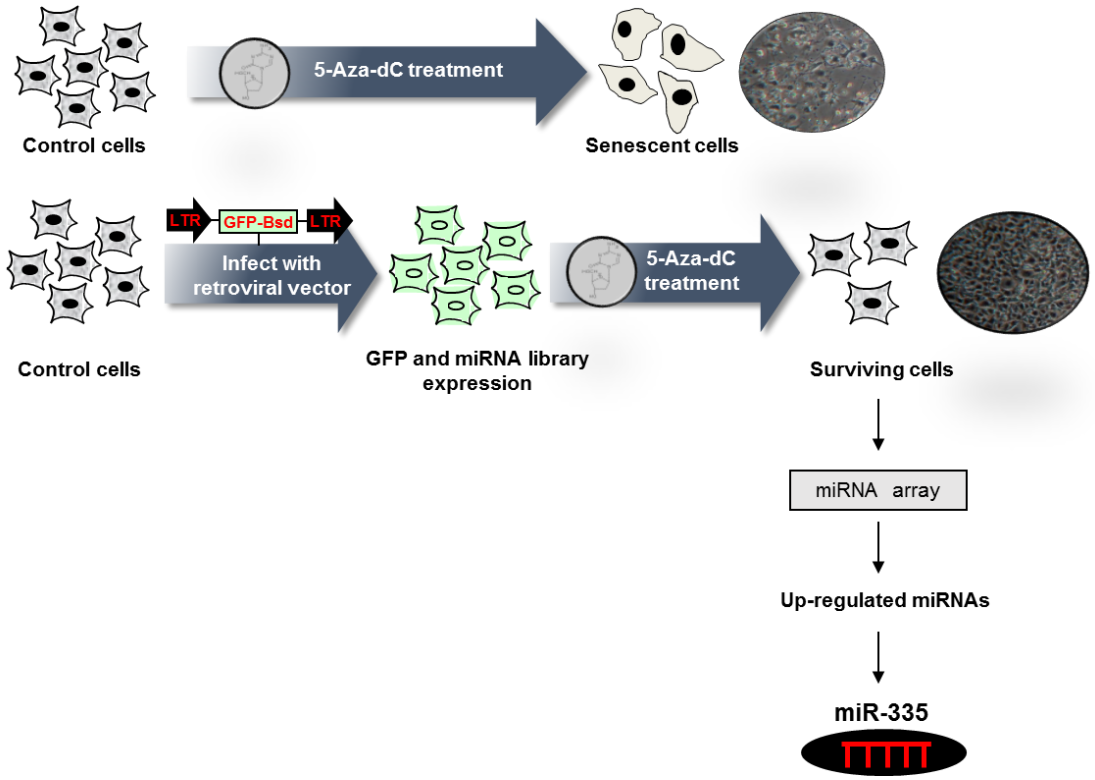

Fig. 3- 1 Identification of miR-335. Strategy for induction of miR library in human cancer cells and loss-of-function screening is described (A). The cells infected with bicistronic vector constituting of two promoters and GFP were treated with 5-Aza-dC. Whereas control uninfected cells showed induction of senescence, colonies emerged in the virus harboring cells. These colonies were expanded and subjected to miR-array analysis with respect to the uninfected control cells. miR array analysis resulted in identification of miR-335 as one of the upregulated miR in cells that escaped 5-Aza-dC induced senescence.

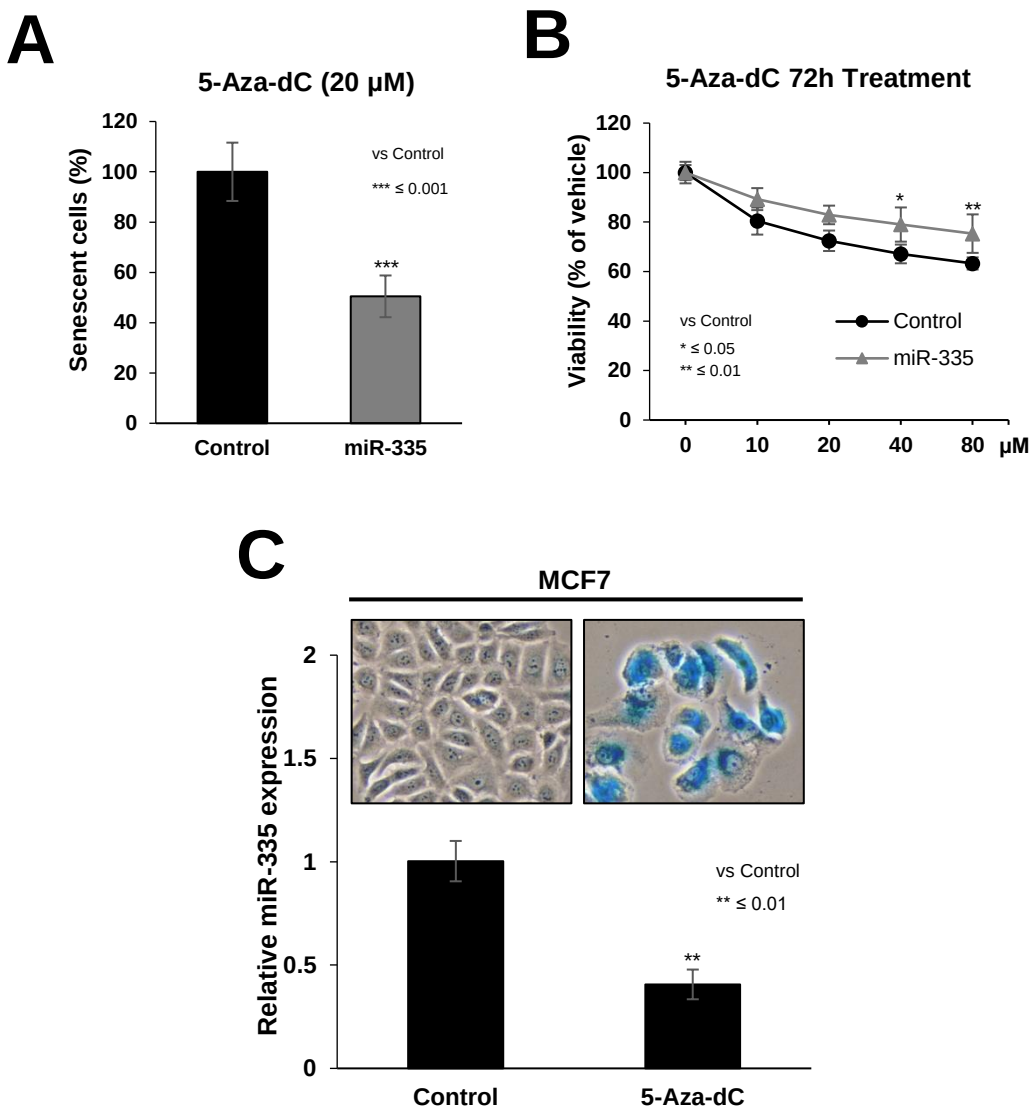

Fig. 3- 2 Cells overexpressing miR-335 showed resistance to 5-Aza-dC induced senescence as examined by senescence associated β-gal staining (A) as well as cell viability assays (B). Cells undergoing 5-Aza-dC induced senescence showed down-regulation of miR-335 (C).

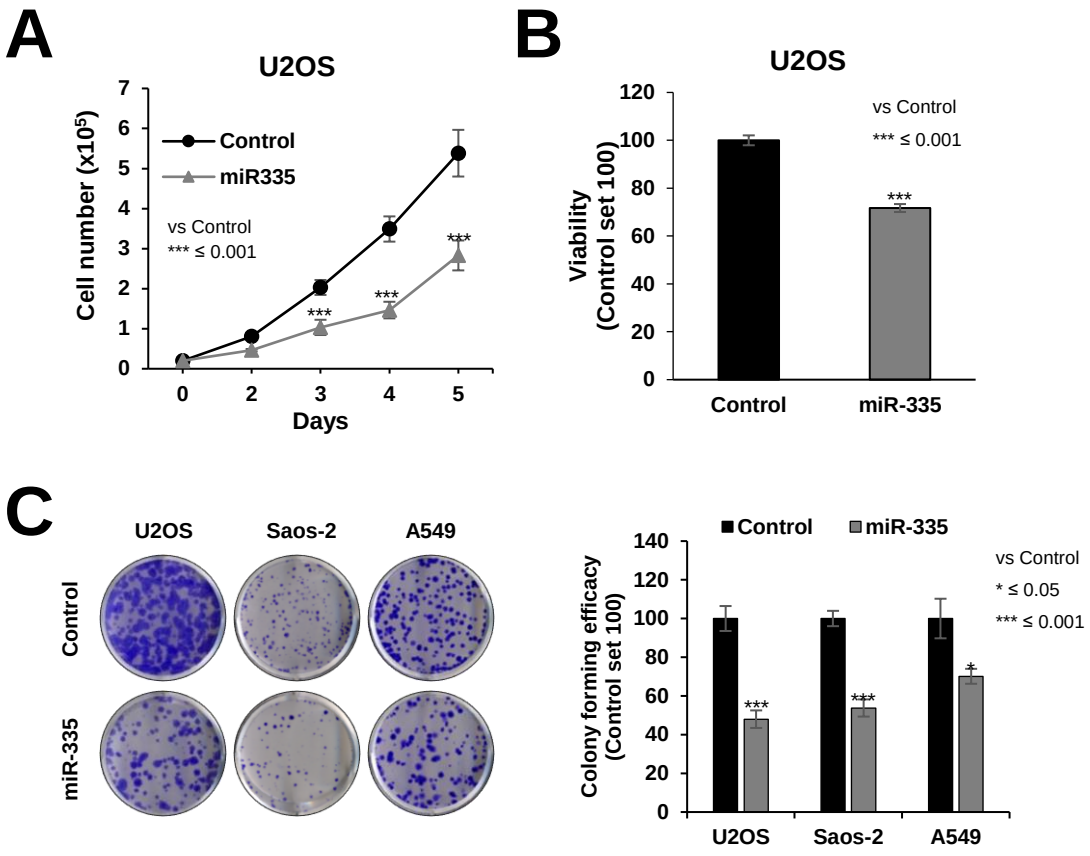

Fig. 3- 3 Growth curve of control and miR-335 overexpressing cells showed slower growth of the latter (A). Short and long term survival by viability analysis (B) and colony forming assay (C) showed about 30% and 50% reduction, respectively.

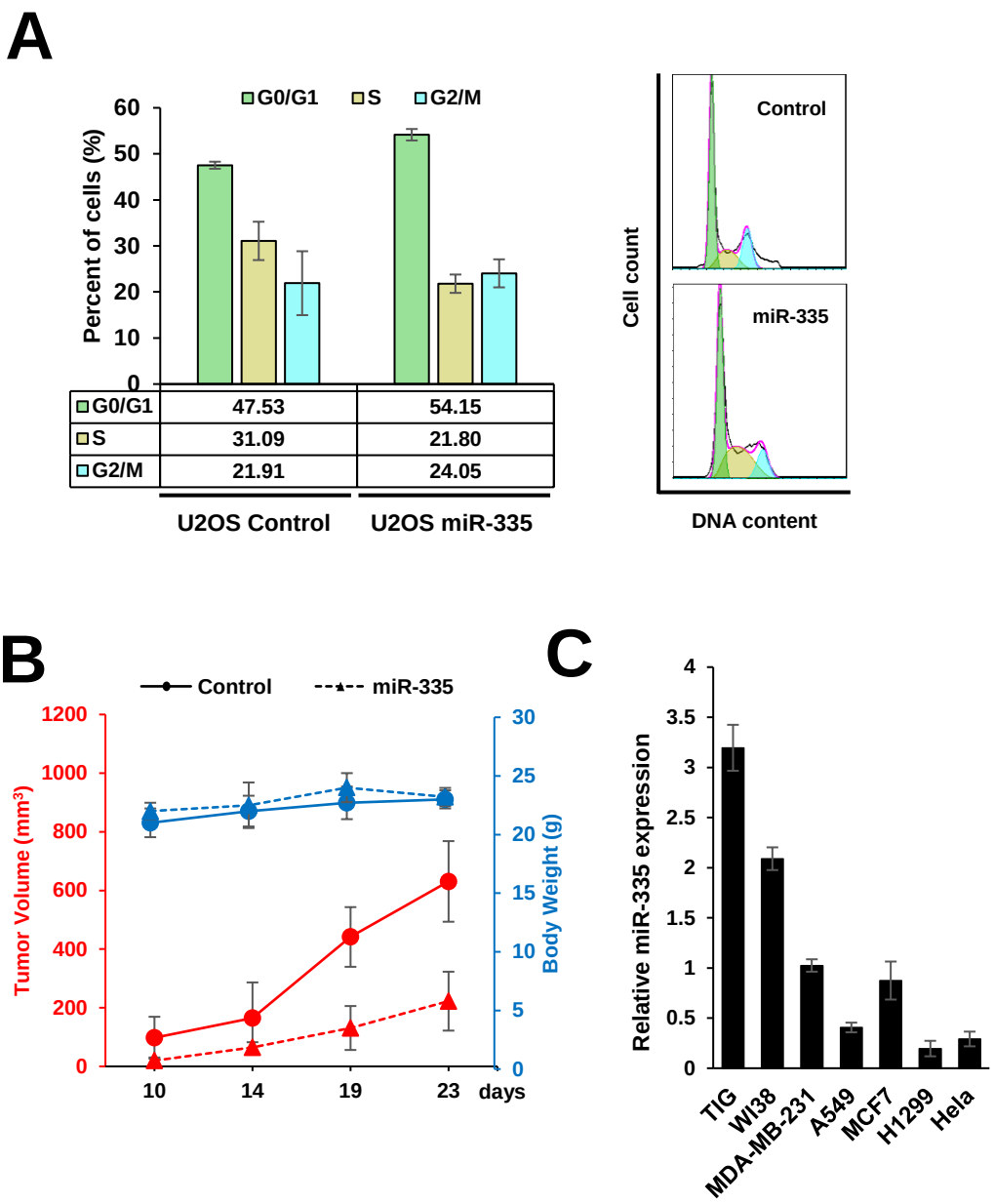

Fig. 3- 4 Cell cycle analysis showed increase in number of cells at G0/G1, and decrease in S phase (A). miR-335 overexpressing cells, in subcutaneous xenografts in nude mice, showed low tumor forming capacity as compared to the control cells. Body weight of the mice during the course of experiment showed no difference (B). Expression analysis of miR-335 in human normal and cancer cells showed its higher level of expression in normal cells (C).

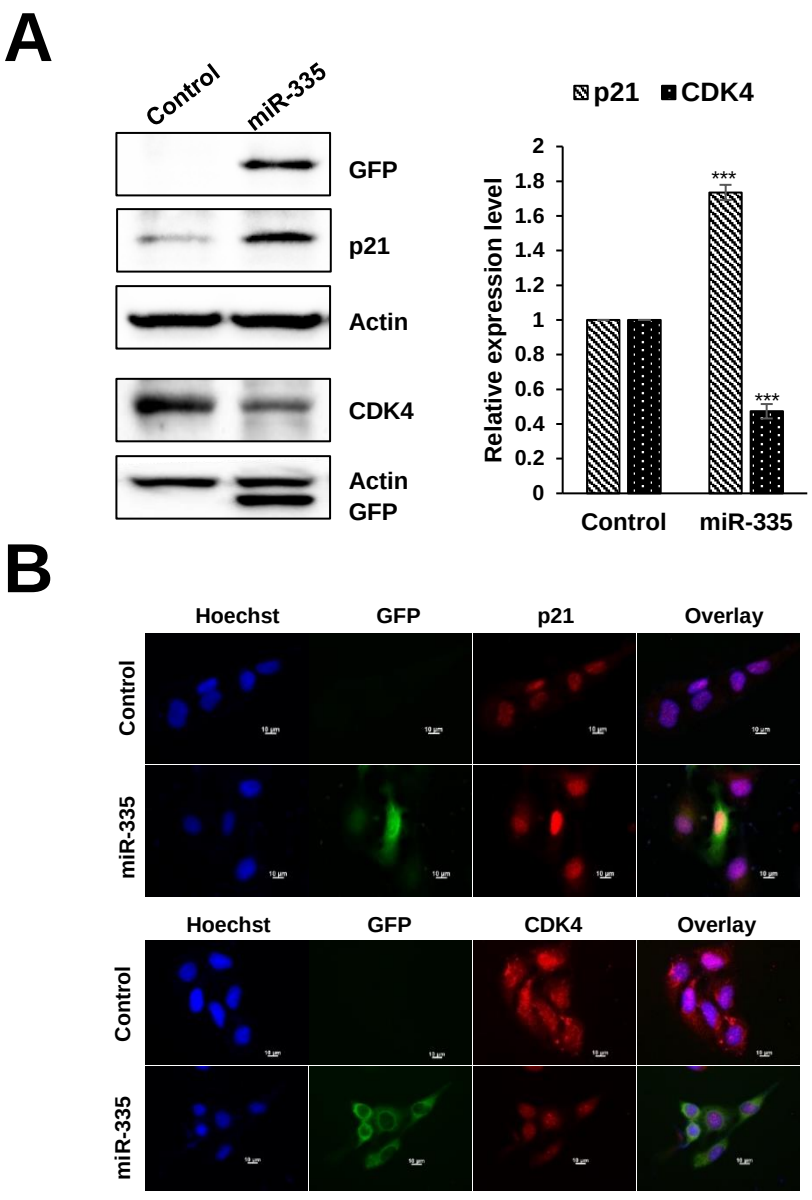

Fig. 3-5 Western blotting (A) and immunostaining (B) showed miR-335 overexpressing cells possessed higher level of expression of $p21^{WAF1}$, and low level of expression of CDK4. Scale bar = 30 μm.

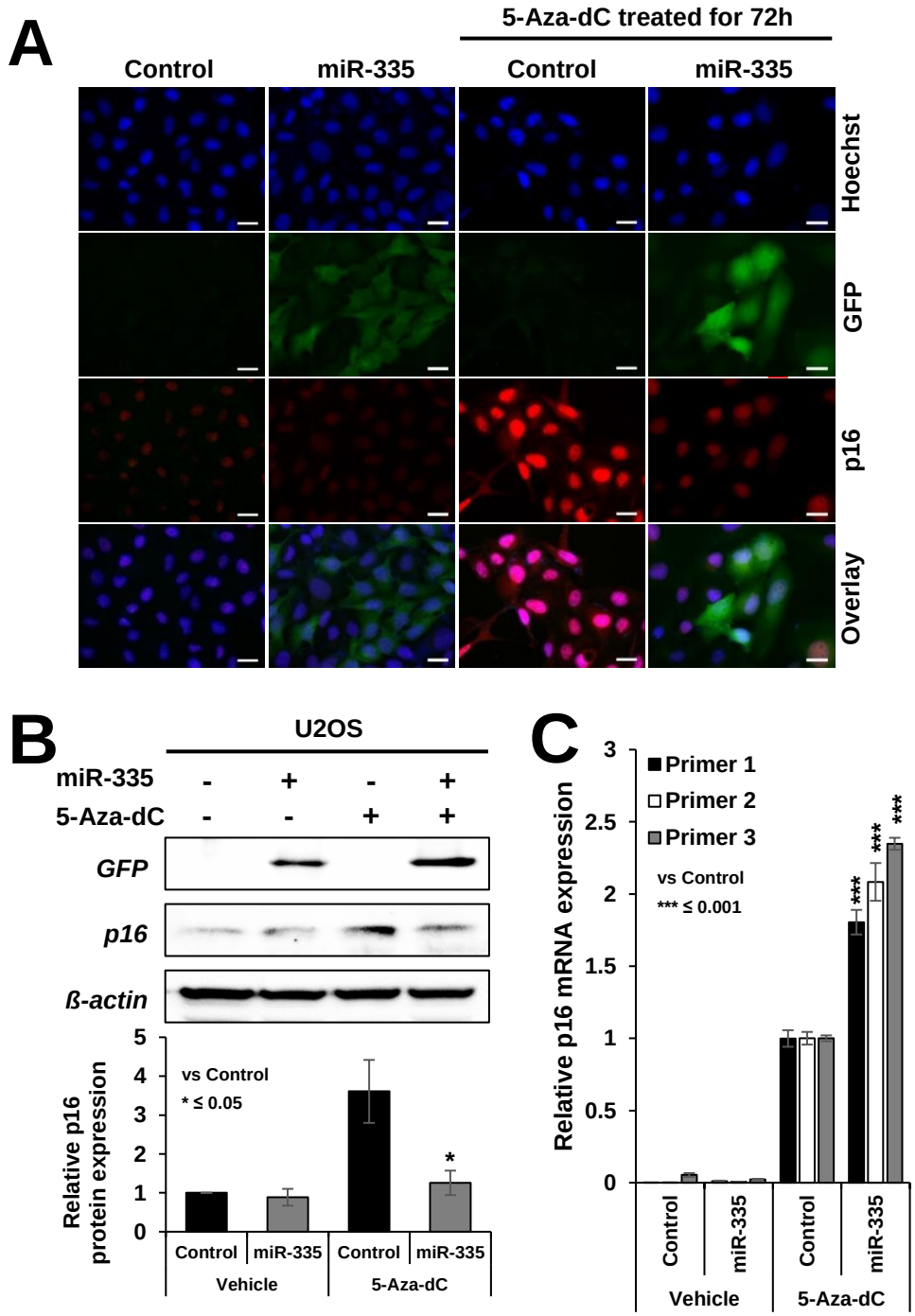

Fig. 3- 6 Immunostaining (A) and Western blotting (B) of control, miR-335-transfected cells treated with 5Aza-dC showed that the latter caused increase in expression of $p16^{INK4A}$ and miR-335 compromised $p16^{INK4A}$ increase at the protein (A and B), but not mRNA level (C). miR-335 transfected and 5Aza-dC treated cells showed increase in $p16^{INK4A}$ transcript that was confirmed by three sets of primers. Scale bar = 50 μm.

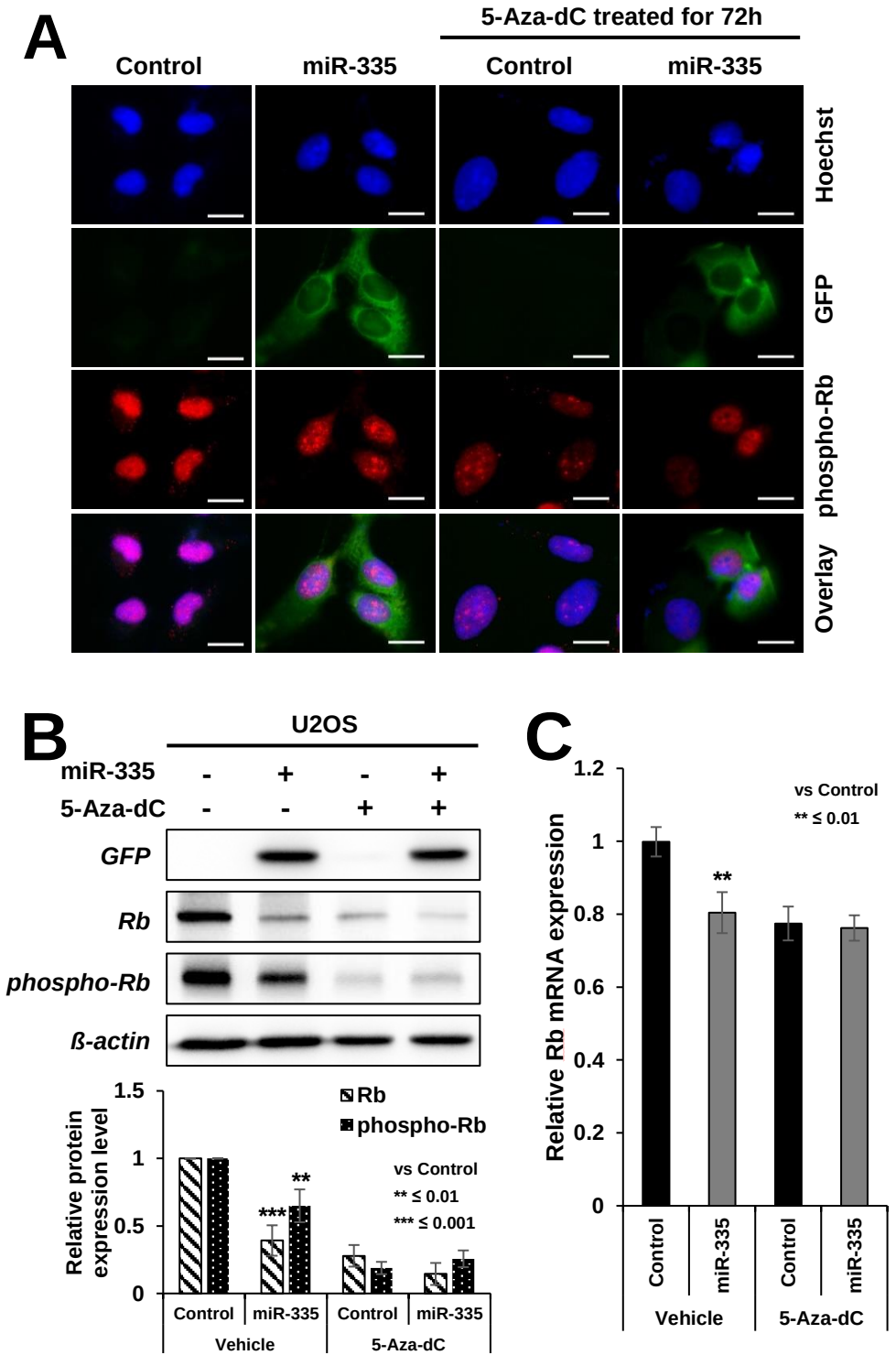

Fig. 3- 7 Immunostaining (A) and Western blotting (B) for pRB in control and miR-335 cells revealed low level of expression of pRB and pRB^{phospho} in the latter. miR-335 transfected cells showed lower level of pRB transcript (C). Scale bar = 20 μm.

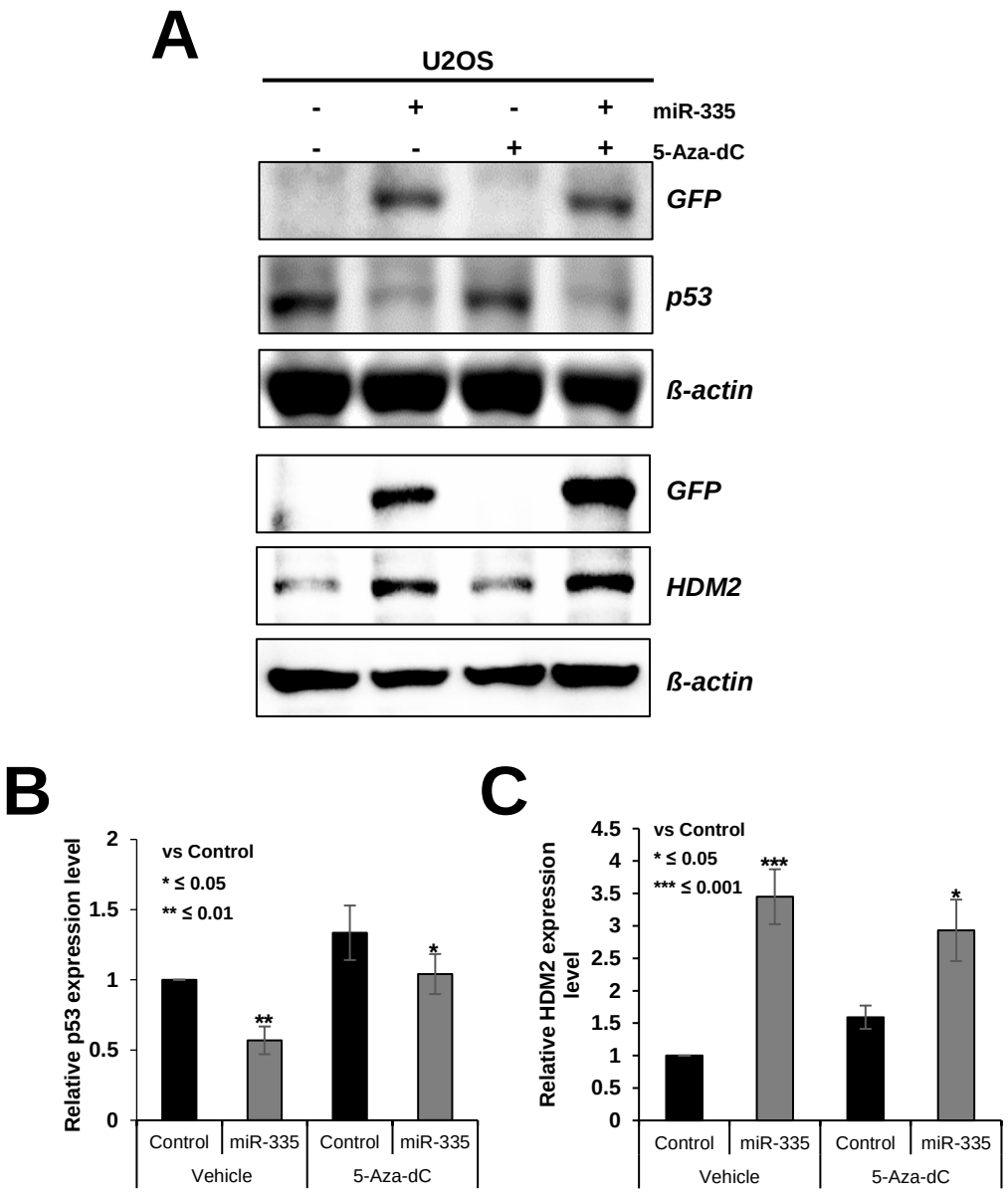

Fig. 3- 8 Western blotting of control and miR-335 cells treated with 5-Aza-dC showed low level of p53 in the latter, 5-Aza-dC increased the p53 expression, HDM2 showed reverse expression as p53 (A). Quantitation of Western blotting data obtained from three independent experiments and the statistical significances are shown (B and C).

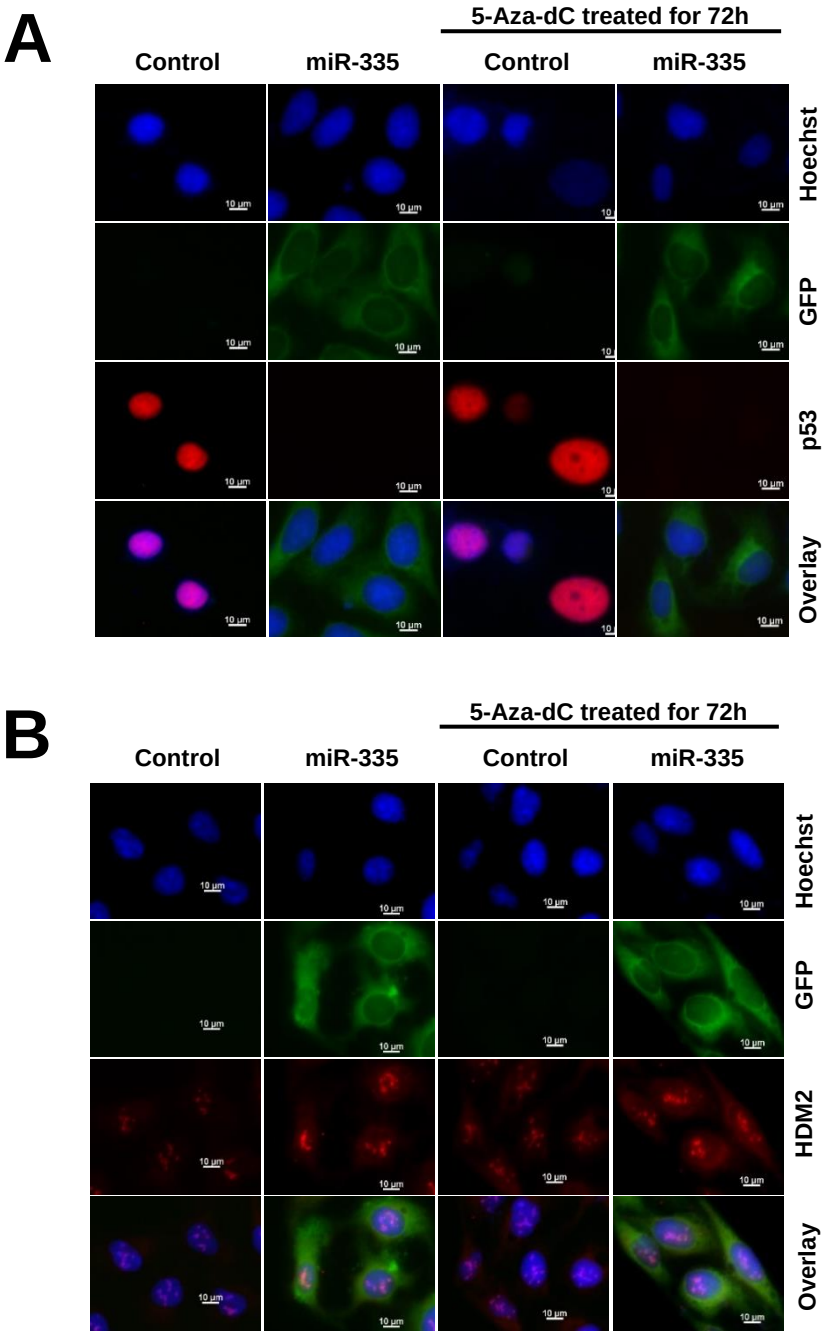

Fig. 3- 9 Imumostaining of control and miR-335 cells treated with 5-Aza-dC showed low level of p53 in the latter, 5-Aza-dC increased the p53 expression (A), HDM2 showed reverse expression as p53 (B).

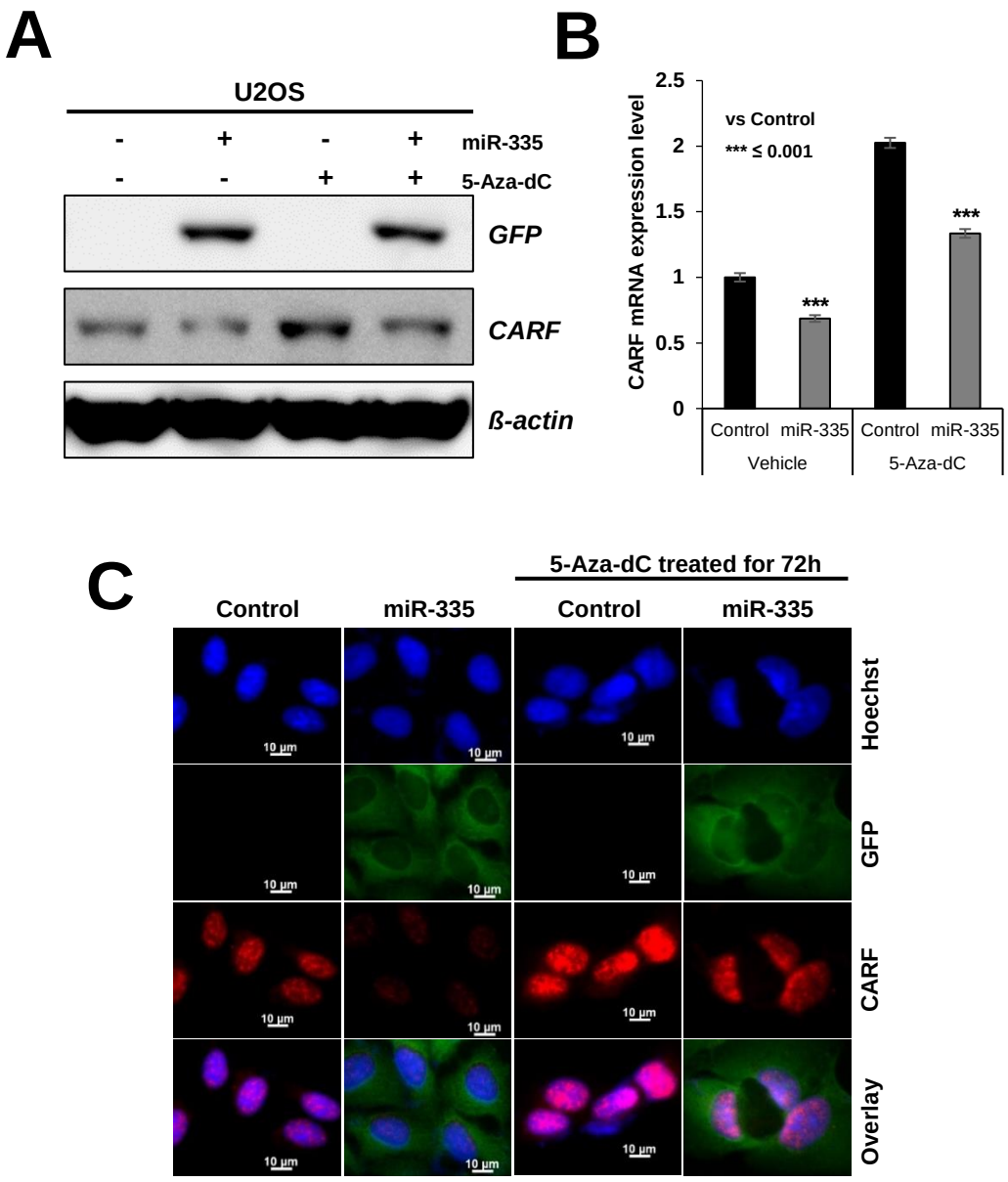

Fig. 3- 10 Western blotting (A), qRT-PCR (B) and immunostaining (C) for CARF showed decreased level of expression in miR-335 overexpressing cells.

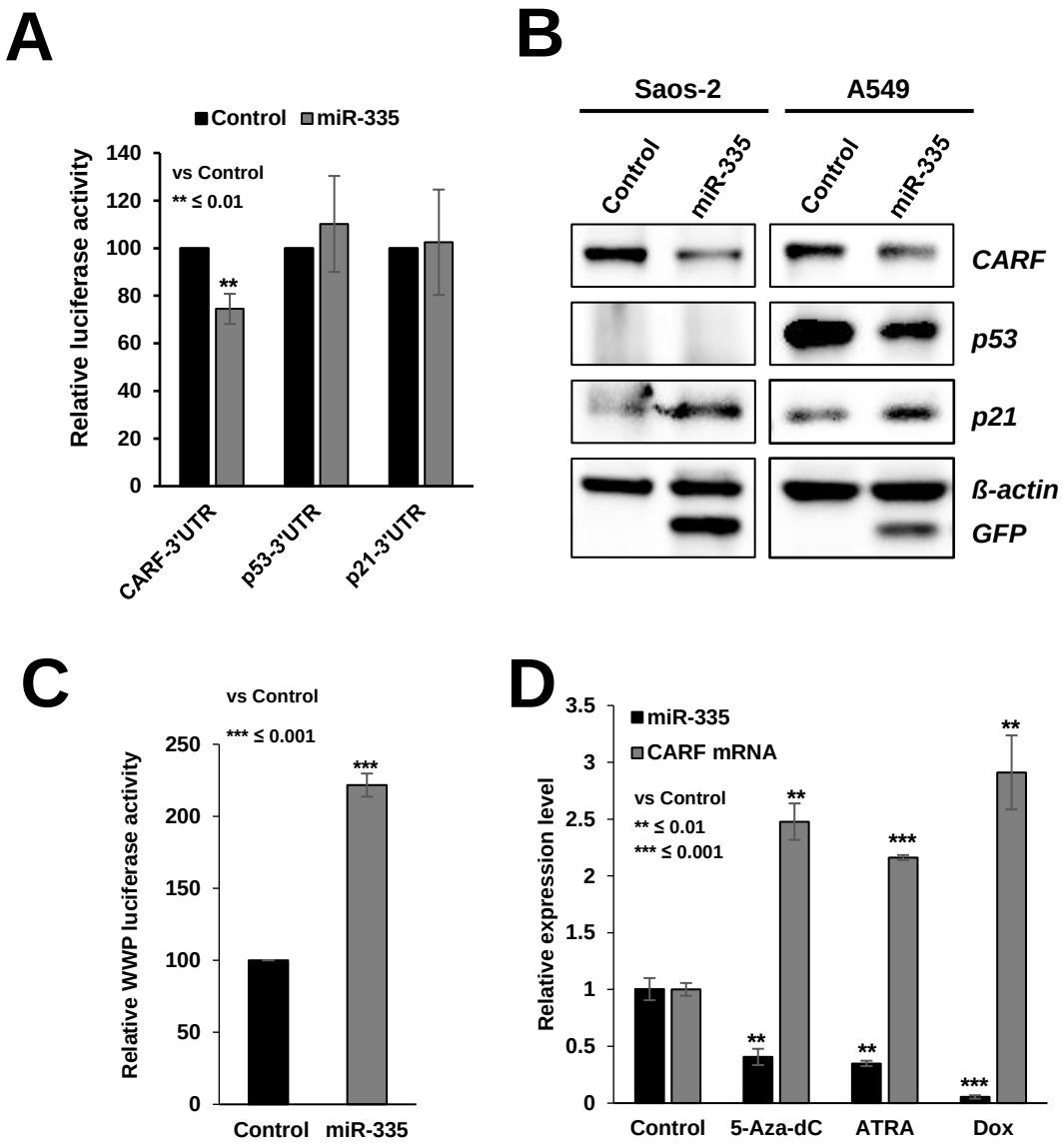

Fig. 3- 11 3'UTR reporter assay for CARF, p53 and p21 in control and miR-335 overexpressing cells showed that miR-335 targets CARF (A). Increase in $p21^{WAF1}$ occurred in p53-/- cells and was hence independent to that of p53 (B). $p21^{WAF1}$ promoter reporter assay in control and miR-335 transfected cells showed upregulation of p21 (C). Cells undergoing growth arrest by retinoic acid (ATRA) and doxorubicin (Dox) showed decrease in miR-335 and increase in CARF expression; 5Aza-dC was used as a control for comparison (D).

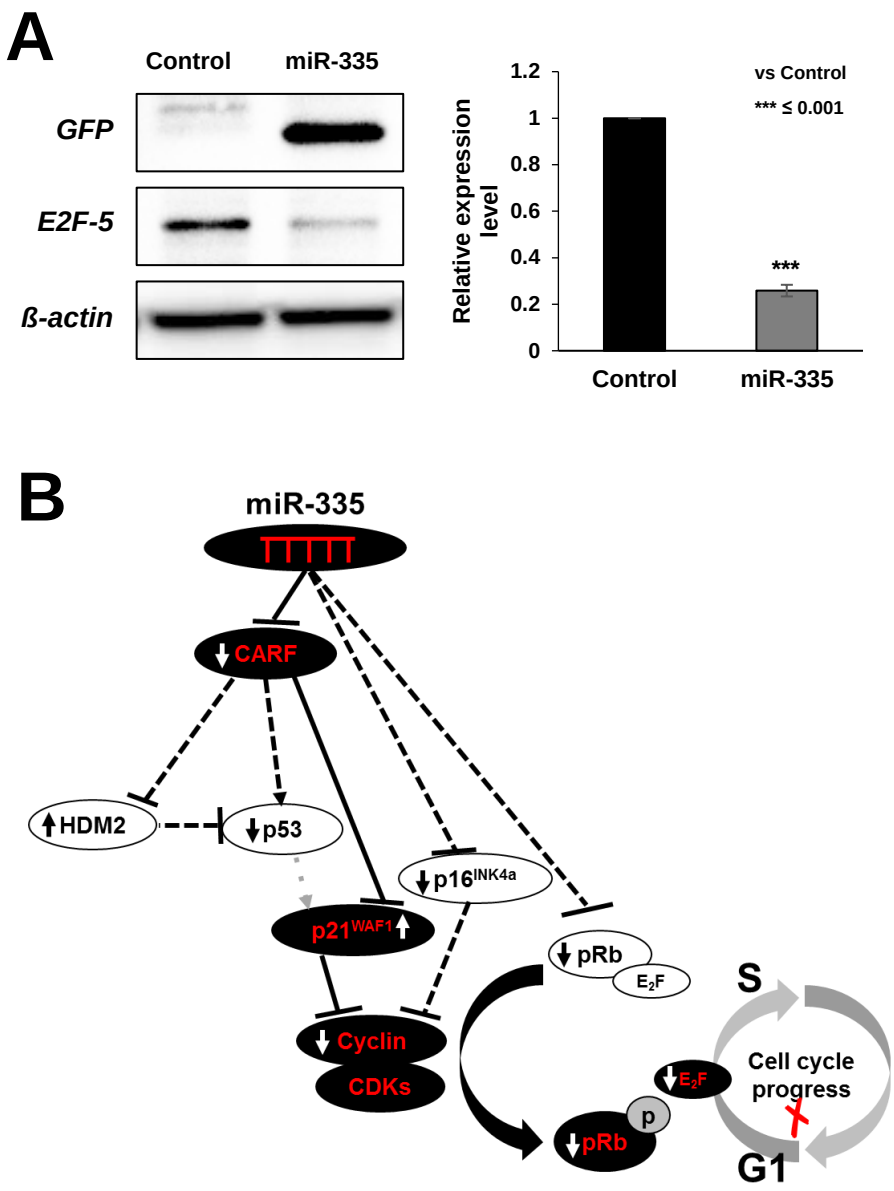

Fig. 3- 12 miR-335 transfected cells showed low expression level of E_2F-5 than control cells (A). Schematic presentation of miR-335 targets as resolved in this study. Dominant pathways are shown by solid lines. Upregulation and downregulation of proteins are shown by upward and downward arrows (B).

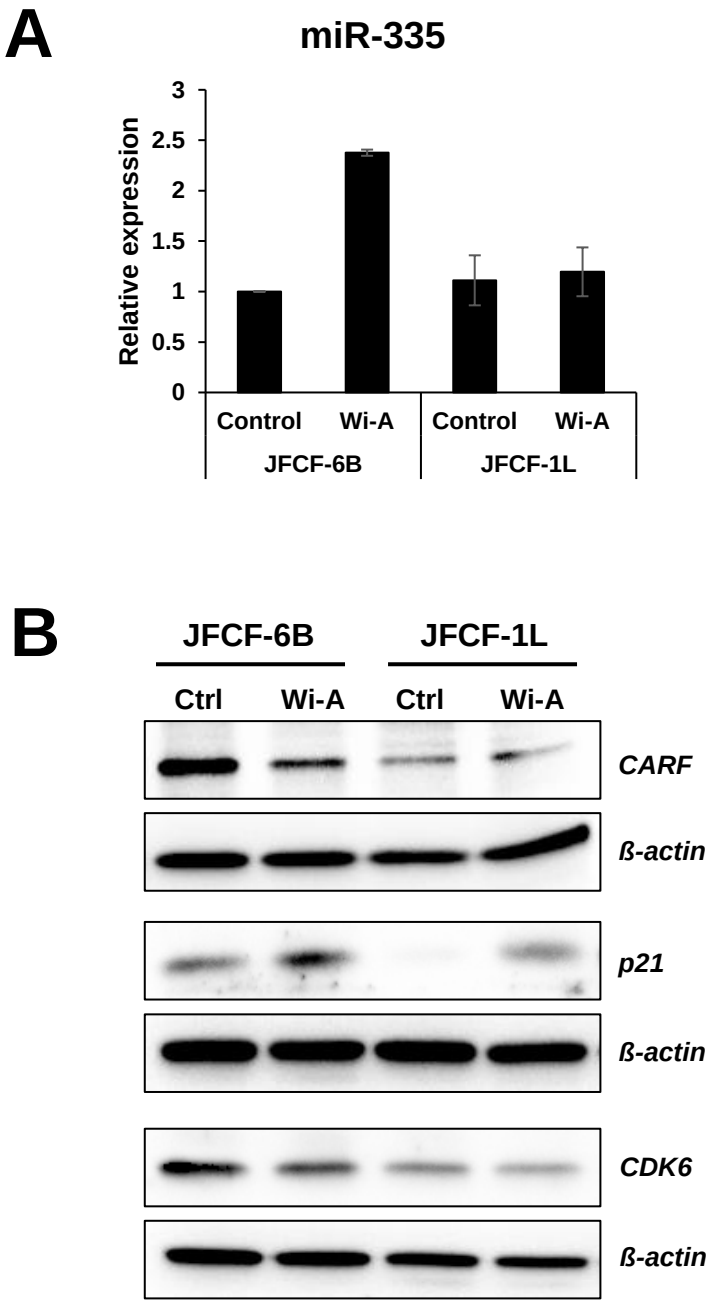

Fig. 3- 13 Telomerase positive JFCF-6B cell showed higher miR-335 expression in response to Wi-A treatment (A). Hence, in JFCF-6B cell, Wi-A treatment led to down-regulated of CARF and CDK6, up-regulated of p21, whereas JFCF-1L was relatively less affected because of low level of CARF expression (B).

Chapter 4 Conclusions and future research

Each of the ~10^3 human cells receives tens of thousands of DNA lesions per day. To counter this threat, life has evolved several systems to mediate its repair. However, if the cells are not repair or repair incorrectly, they lead to mutations or wide-scale genome aberrations that results in tumorigenesis. Today, Cancer has been on the rise since the average human lifespan has increased so dramatically over the last century. The development of industrialization and unhealthy lifestyles also increase the incidence of this disease. Although advancements in diagnostic and therapeutic technologies have improved cancer survival statistics, 75% of the world population live in developing country and have poor access to the advanced remedies. Natural plant therapies, like Ashwagandha, hence become an alternative choice for treatment. We aim to study anticancer activity of Withaferin A (extract from Ashugandha leaf) in aspects of telomere maintenance and mircoRNA regulation.

4.1 Conclusions

In this thesis, we used isogenic cells with or without telomerase and found that:

1. Wi-A caused stronger cytotoxity to ALT cells. The G2/M arrest and apoptosis resulting from Wi-A exposure was specific to ALT cells.
2. Treatment with Wi-A decreased in the number of ALT-associated promyelocytic leukemia (PML) nuclear bodies (APBs) (a universal characterization of ALT), whereas telomerase activity was unaffected.
3. ALT cells treated with Wi-A exhibited severe telomere dysfunction and upregulation of DNA damage response.
4. Molecular analysis revealed that treatment with Wi-A lead to Myc- mediated transcriptional suppression of MRN complex, which is essential for ALT mechanism and cell survival.

In the meanwhile, we recruited arbitrary manipulation of genome and escape from 5-Aza-2'-deoxycytidine (5-Aza-dC) induced senescence as a cell based loss-of-function

screening system. Cells that escaped 5-Aza-dC induced senescence were recovered and subjected to miR-microarray analysis with respect to the untreated control. We identified that:

1. miR-335 as one of the upregulated miRs in the cells that escaped 5-Aza-dC induced senescence.
2. miR-335 overexpression in a variety of human cancer cells with either telomerase or ALT mechanism causes growth arrest and hence inhibited incorporation of 5-Aza-dC enabling cells to escape induction of senescence.
3. miR-335 targets multiple proteins including $p16^{INK4A}$, pRB and CARF (Collaborator of ARF) and causes growth arrest of cancer cells by complex interactions of its gene targets.
4. miR-335 expression is increased by Wi-A treatment in telomerase cells, inducing CARF mediated cellular growth arrest.

Collectively, this study provide a new strategy for the development of Wi-A based drug screening and designing in the future.

4.2 Future work

1. In spite of the obstacle that ALT cells don't form xenograft tumor, Wi-A effect on telomerase/ALT or miRNA-335 should be confirmed by *in vivo* or *ex vivo* study
2. The top Wi-A targeted molecule(s) in cancer cells needs to be identified. This will ultimately help to understand the underlying mechnism.

Acknowledgments

Though only my name appears on the cover of this dissertation, a great many people have contributed to its production. I owe my gratitude to all those people who have made this dissertation possible and because of whom my graduate experience has been one that I will cherish forever.

First and Foremost, I would like to express my sincere gratitude to Prof. Zhenya Zhang, Prof. Renu Wadhwa and Prof. Sunil kaul for the continuous support for my study and research.

I would further like to express my great appreciation to my thesis committee for their valuable and insightful comments, which helped me in improving this thesis. Special gratitude is expressed to Associate Prof. Zhongfang Lei and Asscociate Prof. Keiko Yamaji for their encouragement and kind help during my Ph. D studies.

Many thanks to my dear friends and lab mates Dr. Ran Gao, Dr. Jihoon Ryu, Dr. Chuan Huang, Dr. Nupur Nigam, Mr. Wei Cai, Ms. Xi Yang, Ms. Ling Li, and many others for their friendship and countless help during the last three years.

I appreciate the financial support from China Scholarship Council (CSC) helped make the completion of my graduate work possible.

Last but not least, I would like to especially thank my wife and my parents. Words alone cannot express what I owe you for your encouragement and patient love, which enabled me to complete my study.

References

[1] Arseculeratne S N, Gunatilaka A A, Panabokke R G. Studies of medicinal plants of Sri Lanka. Part 14: Toxicity of some traditional medicinal herbs. J Ethnopharmacol, 1985, 13(3): 323-335.

[2] Singh N, Bhalla M, De Jager P, et al. An overview on ashwagandha: a Rasayana (rejuvenator) of Ayurveda. Afr J Tradit Complement Altern Med, 2011, 8(5 Suppl): 208-213.

[3] Bhattacharya S K, Muruganandam A V. Adaptogenic activity of Withania somnifera: an experimental study using a rat model of chronic stress. Pharmacol Biochem Behav, 2003, 75(3): 547-555.

[4] Dar N J, Hamid A, Ahmad M. Pharmacologic overview of Withania somnifera, the Indian Ginseng. Cell Mol Life Sci, 2015, 72(23): 4445-4460.

[5] Mishra L C, Singh B B, Dagenais S. Scientific basis for the therapeutic use of Withania somnifera (ashwagandha): a review. Altern Med Rev, 2000, 5(4): 334-346.

[6] Vanden Berghe W, Sabbe L, Kaileh M, et al. Molecular insight in the multifunctional activities of Withaferin A. Biochemical Pharmacology, 2012, 84(10): 1282-1291.

[7] Lv T Z, Wang G S. Antiproliferation potential of withaferin A on human osteosarcoma cells via the inhibition of G2/M checkpoint proteins. Exp Ther Med, 2015, 10(1): 323-329.

[8] Kim J H, Kim S J. Overexpression of microRNA-25 by withaferin A induces cyclooxygenase-2 expression in rabbit articular chondrocytes. J Pharmacol Sci, 2014, 125(1): 83-90.

[9] Munagala R, Kausar H, Munjal C, et al. Withaferin A induces p53-dependent apoptosis by repression of HPV oncogenes and upregulation of tumor suppressor proteins in human cervical cancer cells. Carcinogenesis, 2011, 32(11): 1697-1705.

[10] Srinivasan S, Ranga R S, Burikhanov R, et al. Par-4-dependent apoptosis by the dietary compound withaferin A in prostate cancer cells. Cancer Res, 2007, 67(1): 246-253.

[11] Choi S, Singh S V. Bax and Bak are required for apoptosis induction by sulforaphane, a cruciferous vegetable-derived cancer chemopreventive agent. Cancer Res, 2005, 65(5): 2035-2043.

[12] Gao R, Shah N, Lee J S, et al. Withanone-rich combination of Ashwagandha withanolides restricts metastasis and angiogenesis through hnRNP-K. Mol Cancer Ther, 2014, 13(12): 2930-2940.

[13] Thaiparambil J T, Bender L, Ganesh T, et al. Withaferin A inhibits breast cancer invasion and metastasis at sub-cytotoxic doses by inducing vimentin disassembly and serine 56 phosphorylation. Int J Cancer, 2011, 129(11): 2744-2755.

[14] Shay J W, Wright W E. Telomerase activity in human cancer. Curr Opin Oncol, 1996, 8(1): 66-71.

[15] Griffith J D, Comeau L, Rosenfield S, et al. Mammalian telomeres end in a large duplex loop. Cell, 1999, 97(4): 503-514.

[16] Greider C W. Telomeres do D-loop-T-loop[J]. Cell, 1999, 97(4): 419-422.

[17] Lipps H J, Rhodes D. G-quadruplex structures: in vivo evidence and function. Trends Cell Biol, 2009, 19(8): 414-422.

[18] Ye J Z, Donigian J R, Van Overbeek M, et al. TIN2 binds TRF1 and TRF2 simultaneously and stabilizes the TRF2 complex on telomeres. J Biol Chem, 2004, 279(45): 47264-47271.

[19] Baumann P, Cech T R. Pot1, the putative telomere end-binding protein in fission yeast and humans. Science, 2001, 292(5519): 1171-1175.

[20] Sfeir A, Kosiyatrakul S T, Hockemeyer D, et al. Mammalian telomeres resemble fragile sites and require TRF1 for efficient replication. Cell, 2009, 138(1): 90-103.

[21] Van Steensel B, Smogorzewska A, De Lange T. TRF2 protects human telomeres from end-to-end fusions. Cell, 1998, 92(3): 401-413.

[22] Loayza D, De Lange T. POT1 as a terminal transducer of TRF1 telomere length control. Nature, 2003, 423(6943): 1013-1018.

[23] Liu D, O'connor M S, Qin J, et al. Telosome, a mammalian telomere-associated complex formed by multiple telomeric proteins. J Biol Chem, 2004, 279(49): 51338-51342.

[24] Denchi E L, De Lange T. Protection of telomeres through independent control of ATM and ATR by TRF2 and POT1. Nature, 2007, 448(7157): 1068-1071.

[25] Celli G B, De Lange T. DNA processing is not required for ATM-mediated telomere damage response after TRF2 deletion. Nat Cell Biol, 2005, 7(7): 712-718.

[26] Zhang J, Rane G, Dai X, et al. Ageing and the telomere connection: An intimate relationship with inflammation. Ageing Res Rev, 2016, 25: 55-69.

[27] Venkatesan S, Natarajan A T, Hande M P. Chromosomal instability--mechanisms and consequences.

Mutat Res Genet Toxicol Environ Mutagen, 2015, 793: 176-184.

[28] Buseman C M, Wright W E, Shay J W. Is telomerase a viable target in cancer? Mutat Res, 2012, 730(1-2): 90-97.

[29] Shore D, Bianchi A. Telomere length regulation: coupling DNA end processing to feedback regulation of telomerase. EMBO J, 2009, 28(16): 2309-2322.

[30] Harley C B. Telomere loss: mitotic clock or genetic time bomb? Mutat Res, 1991, 256(2-6): 271-282.

[31] Collins K, Mitchell J R. Telomerase in the human organism. Oncogene, 2002, 21(4): 564-579.

[32] Cesare A J, Reddel R R. Alternative lengthening of telomeres: models, mechanisms and implications. Nat Rev Genet, 2010, 11(5): 319-330.

[33] Nakamura T M, Morin G B, Chapman K B, et al. Telomerase catalytic subunit homologs from fission yeast and human. Science, 1997, 277(5328): 955-959.

[34] Meyerson M, Counter C M, Eaton E N, et al. hEST2, the putative human telomerase catalytic subunit gene, is up-regulated in tumor cells and during immortalization. Cell, 1997, 90(4): 785-795.

[35] Harrington L, Zhou W, Mcphail T, et al. Human telomerase contains evolutionarily conserved catalytic and structural subunits. Genes Dev, 1997, 11(23): 3109-3115.

[36] Takakura M, Kyo S, Kanaya T, et al. Expression of human telomerase subunits and correlation with telomerase activity in cervical cancer. Cancer Res, 1998, 58(7): 1558-1561.

[37] Cohen S B, Graham M E, Lovrecz G O, et al. Protein composition of catalytically active human telomerase from immortal cells. Science, 2007, 315(5820): 1850-1853.

[38] Gellert G C, Dikmen Z G, Wright W E, et al. Effects of a novel telomerase inhibitor, GRN163L, in human breast cancer. Breast Cancer Res Treat, 2006, 96(1): 73-81.

[39] Dikmen Z G, Gellert G C, Jackson S, et al. In vivo inhibition of lung cancer by GRN163L: a novel human telomerase inhibitor. Cancer Res, 2005, 65(17): 7866-7873.

[40] Gu J, Andreeff M, Roth J A, et al. hTERT promoter induces tumor-specific Bax gene expression and cell killing in syngenic mouse tumor model and prevents systemic toxicity. Gene Ther, 2002, 9(1): 30-37.

[41] Majumdar A S, Hughes D E, Lichtsteiner S P, et al. The telomerase reverse transcriptase promoter

drives efficacious tumor suicide gene therapy while preventing hepatotoxicity encountered with constitutive promoters. Gene Ther, 2001, 8(7): 568-578.

[42] Abdul-Ghani R, Ohana P, Matouk I, et al. Use of transcriptional regulatory sequences of telomerase (hTER and hTERT) for selective killing of cancer cells. Mol Ther, 2000, 2(6): 539-544.

[43] Kotsakis A, Vetsika E K, Christou S, et al. Clinical outcome of patients with various advanced cancer types vaccinated with an optimized cryptic human telomerase reverse transcriptase (TERT) peptide: results of an expanded phase II study. Ann Oncol, 2012, 23(2): 442-449.

[44] Inderberg-Suso E M, Trachsel S, Lislerud K, et al. Widespread CD4+ T-cell reactivity to novel hTERT epitopes following vaccination of cancer patients with a single hTERT peptide GV1001. Oncoimmunology, 2012, 1(5): 670-686.

[45] Brunsvig P F, Aamdal S, Gjertsen M K, et al. Telomerase peptide vaccination: a phase I/II study in patients with non-small cell lung cancer. Cancer Immunol Immunother, 2006, 55(12): 1553-1564.

[46] Wang R C, Smogorzewska A, De Lange T. Homologous recombination generates T-loop-sized deletions at human telomeres. Cell, 2004, 119(3): 355-368.

[47] Yeager T R, Neumann A A, Englezou A, et al. Telomerase-negative immortalized human cells contain a novel type of promyelocytic leukemia (PML) body. Cancer Res, 1999, 59(17): 4175-4179.

[48] Bryan T M, Englezou A, Gupta J, et al. Telomere elongation in immortal human cells without detectable telomerase activity. EMBO J, 1995, 14(17): 4240-4248.

[49] Murnane J P, Sabatier L, Marder B A, et al. Telomere dynamics in an immortal human cell line. EMBO J, 1994, 13(20): 4953-4962.

[50] Henson J D, Cao Y, Huschtscha L I, et al. DNA C-circles are specific and quantifiable markers of alternative-lengthening-of-telomeres activity. Nat Biotechnol, 2009, 27(12): 1181-1185.

[51] Lovejoy C A, Li W, Reisenweber S, et al. Loss of ATRX, genome instability, and an altered DNA damage response are hallmarks of the alternative lengthening of telomeres pathway. PLoS Genet, 2012, 8(7): e1002772.

[52] Lewis P W, Elsaesser S J, Noh K M, et al. Daxx is an H3.3-specific histone chaperone and cooperates with ATRX in replication-independent chromatin assembly at telomeres. Proc Natl Acad Sci U S A, 2010, 107(32): 14075-14080.

[53] Henson J D, Reddel R R. Assaying and investigating Alternative Lengthening of Telomeres activity in human cells and cancers. FEBS Lett, 2010, 584(17): 3800-3811.

[54] Goldberg A D, Banaszynski L A, Noh K M, et al. Distinct factors control histone variant H3.3 localization at specific genomic regions. Cell, 2010, 140(5): 678-691.

[55] Jiang W Q, Zhong Z H, Henson J D, et al. Suppression of alternative lengthening of telomeres by Sp100-mediated sequestration of the MRE11/RAD50/NBS1 complex. Mol Cell Biol, 2005, 25(7): 2708-2721.

[56] Bailey S M, Brenneman M A, Goodwin E H. Frequent recombination in telomeric DNA may extend the proliferative life of telomerase-negative cells. Nucleic Acids Res, 2004, 32(12): 3743-3751.

[57] Cesare A J, Kaul Z, Cohen S B, et al. Spontaneous occurrence of telomeric DNA damage response in the absence of chromosome fusions. Nat Struct Mol Biol, 2009, 16(12): 1244-1251.

[58] Bucher N, Britten C D. G2 checkpoint abrogation and checkpoint kinase-1 targeting in the treatment of cancer. Br J Cancer, 2008, 98(3): 523-528

[59] Zhong Z H, Jiang W Q, Cesare A J, et al. Disruption of telomere maintenance by depletion of the MRE11/RAD50/NBS1 complex in cells that use alternative lengthening of telomeres. J Biol Chem, 2007, 282(40): 29314-29322.

[60] Lee J H, Paull T T. Activation and regulation of ATM kinase activity in response to DNA double-strand breaks. Oncogene, 2007, 26(56): 7741-7748.

[61] Muntoni A, Neumann A A, Hills M, et al. Telomere elongation involves intra-molecular DNA replication in cells utilizing alternative lengthening of telomeres. Hum Mol Genet, 2009, 18(6): 1017-1027.

[62] Dunham M A, Neumann A A, Fasching C L, et al. Telomere maintenance by recombination in human cells. Nat Genet, 2000, 26(4): 447-450.

[63] Chai W, Sfeir A J, Hoshiyama H, et al. The involvement of the Mre11/Rad50/Nbs1 complex in the generation of G-overhangs at human telomeres. EMBO Rep, 2006, 7(2): 225-230.

[64] Reddel R R. Telomere maintenance mechanisms in cancer: clinical implications. Curr Pharm Des, 2014, 20(41): 6361-6374.

[65] Gocha A R, Nuovo G, Iwenofu O H, et al. Human sarcomas are mosaic for telomerase-dependent

and telomerase-independent telomere maintenance mechanisms: implications for telomere-based therapies. Am J Pathol, 2013, 182(1): 41-48.

[66] Zeng S, Yang Q. The MUS81 endonuclease is essential for telomerase negative cell proliferation. Cell Cycle, 2009, 8(14): 2157-2160.

[67] Zeng S, Xiang T, Pandita T K, et al. Telomere recombination requires the MUS81 endonuclease. Nat Cell Biol, 2009, 11(5): 616-623.

[68] Royle N J, Mendez-Bermudez A, Gravani A, et al. The role of recombination in telomere length maintenance. Biochem Soc Trans, 2009, 37(Pt 3): 589-595.

[69] Bartel D P. MicroRNAs: genomics, biogenesis, mechanism, and function. Cell, 2004, 116(2): 281-297.

[70] Lee R C, Feinbaum R L, Ambros V. The C. elegans heterochronic gene lin-4 encodes small RNAs with antisense complementarity to lin-14. Cell, 1993, 75(5): 843-854.

[71] Griffiths-Jones S, Saini H K, Van Dongen S, et al. miRBase: tools for microRNA genomics. Nucleic Acids Res, 2008, 36(Database issue): D154-158.

[72] Tang G, Reinhart B J, Bartel D P, et al. A biochemical framework for RNA silencing in plants. Genes Dev, 2003, 17(1): 49-63.

[73] Hannon G J. RNA interference. Nature, 2002, 418(6894): 244-251.

[74] Brennecke J, Hipfner D R, Stark A, et al. bantam encodes a developmentally regulated microRNA that controls cell proliferation and regulates the proapoptotic gene hid in Drosophila. Cell, 2003, 113(1): 25-36.

[75] Abrahante J E, Daul A L, Li M, et al. The Caenorhabditis elegans hunchback-like gene lin-57/hbl-1 controls developmental time and is regulated by microRNAs. Dev Cell, 2003, 4(5): 625-637.

[76] Wightman B, Ha I, Ruvkun G. Posttranscriptional regulation of the heterochronic gene lin-14 by lin-4 mediates temporal pattern formation in C. elegans. Cell, 1993, 75(5): 855-862.

[77] Gregory R I, Yan K P, Amuthan G, et al. The Microprocessor complex mediates the genesis of microRNAs. Nature, 2004, 432(7014): 235-240.

[78] Cai X, Hagedorn C H, Cullen B R. Human microRNAs are processed from capped, polyadenylated transcripts that can also function as mRNAs. Rna, 2004, 10(12): 1957-1966.

[79] Lee Y, Ahn C, Han J, et al. The nuclear RNase III Drosha initiates microRNA processing. Nature, 2003, 425(6956): 415-419.

[80] Lee Y, Jeon K, Lee J T, et al. MicroRNA maturation: stepwise processing and subcellular localization. EMBO J, 2002, 21(17): 4663-4670.

[81] Hutvagner G, Mclachlan J, Pasquinelli A E, et al. A cellular function for the RNA-interference enzyme Dicer in the maturation of the let-7 small temporal RNA. Science, 2001, 293(5531): 834-838.

[82] Calin G A, Dumitru C D, Shimizu M, et al. Frequent deletions and down-regulation of micro- RNA genes miR15 and miR16 at 13q14 in chronic lymphocytic leukemia. Proc Natl Acad Sci U S A, 2002, 99(24): 15524-15529.

[83] Michael M Z, Sm O C, Van Holst Pellekaan N G, et al. Reduced accumulation of specific microRNAs in colorectal neoplasia. Mol Cancer Res, 2003, 1(12): 882-891.

[84] Chan J A, Krichevsky A M, Kosik K S. MicroRNA-21 is an antiapoptotic factor in human glioblastoma cells. Cancer Res, 2005, 65(14): 6029-6033.

[85] Feng Z, Zhang C, Wu R, et al. Tumor suppressor p53 meets microRNAs. J Mol Cell Biol, 2011, 3(1): 44-50.

[86] Schwarzenbach H, Nishida N, Calin G A, et al. Clinical relevance of circulating cell-free microRNAs in cancer. Nat Rev Clin Oncol, 2014, 11(3): 145-156.

[87] Manterola L, Guruceaga E, Gallego Perez-Larraya J, et al. A small noncoding RNA signature found in exosomes of GBM patient serum as a diagnostic tool. Neuro Oncol, 2014, 16(4): 520-527.

[88] Bouchie A. First microRNA mimic enters clinic. Nat Biotechnol, 2013, 31(7): 577.

[89] Bader A G. miR-34 - a microRNA replacement therapy is headed to the clinic. Front Genet, 2012, 3: 120.

[90] Wiggins J F, Ruffino L, Kelnar K, et al. Development of a lung cancer therapeutic based on the tumor suppressor microRNA-34. Cancer Res, 2010, 70(14): 5923-5930.

[91] Calado R T, Young N S. Telomere maintenance and human bone marrow failure. Blood, 2008, 111(9): 4446-4455.

[92] Goodall E F, Heath P R, Bandmann O, et al. Neuronal dark matter: the emerging role of microRNAs

in neurodegeneration. Front Cell Neurosci, 2013, 7: 178.

[93] Collado M, Blasco M A, Serrano M. Cellular senescence in cancer and aging. Cell, 2007, 130(2): 223-233.

[94] Artandi S E, Depinho R A. Telomeres and telomerase in cancer. Carcinogenesis, 2010, 31(1): 9-18.

[95] Shay J W, Wright W E. Senescence and immortalization: role of telomeres and telomerase. Carcinogenesis, 2005, 26(5): 867-874.

[96] Shay J W, Wright W E. Role of telomeres and telomerase in cancer. Semin Cancer Biol, 2011, 21(6): 349-353.

[97] Cerni C. Telomeres, telomerase, and myc. An update. Mutat Res, 2000, 462(1): 31-47.

[98] Deng Y, Chan S S, Chang S. Telomere dysfunction and tumour suppression: the senescence connection. Nat Rev Cancer, 2008, 8(6): 450-458.

[99] Osterwald S, Deeg K I, Chung I, et al. PML induces compaction, TRF2 depletion and DNA damage signaling at telomeres and promotes their alternative lengthening. J Cell Sci, 2015, 128(10): 1887-1900.

[100] Venturini L, Erdas R, Costa A, et al. ALT-associated promyelocytic leukaemia body (APB) detection as a reproducible tool to assess alternative lengthening of telomere stability in liposarcomas. J Pathol, 2008, 214(4): 410-414.

[101] Brachner A, Sasgary S, Pirker C, et al. Telomerase- and alternative telomere lengthening-independent telomere stabilization in a metastasis-derived human non-small cell lung cancer cell line: effect of ectopic hTERT. Cancer Res, 2006, 66(7): 3584-3592.

[102] Lundblad V. Telomere maintenance without telomerase. Oncogene, 2002, 21(4): 522-531.

[103] Kumakura S, Tsutsui T W, Yagisawa J, et al. Reversible conversion of immortal human cells from telomerase-positive to telomerase-negative cells. Cancer Res, 2005, 65(7): 2778-2786.

[104] Cerone M A, Londono-Vallejo J A, Bacchetti S. Telomere maintenance by telomerase and by recombination can coexist in human cells. Hum Mol Genet, 2001, 10(18): 1945-1952.

[105] Shay J W, Bacchetti S. A survey of telomerase activity in human cancer. Eur J Cancer, 1997, 33(5): 787-791.

[106] Bryan T M, Englezou A, Dalla-Pozza L, et al. Evidence for an alternative mechanism for

maintaining telomere length in human tumors and tumor-derived cell lines. Nat Med, 1997, 3(11): 1271-1274.

[107] Venturini L, Motta R, Gronchi A, et al. Prognostic relevance of ALT-associated markers in liposarcoma: a comparative analysis. BMC Cancer, 2010, 10: 254.

[108] Wang N, Xu D, Sofiadis A, et al. Telomerase-dependent and independent telomere maintenance and its clinical implications in medullary thyroid carcinoma. J Clin Endocrinol Metab, 2014, 99(8): E1571-1579.

[109] Lamarche B J, Orazio N I, Weitzman M D. The MRN complex in double-strand break repair and telomere maintenance. FEBS Lett, 2010, 584(17): 3682-3695.

[110] Lee J H, Mand M R, Deshpande R A, et al. Ataxia telangiectasia-mutated (ATM) kinase activity is regulated by ATP-driven conformational changes in the Mre11/Rad50/Nbs1 (MRN) complex. J Biol Chem, 2013, 288(18): 12840-12851.

[111] Lavin M F, Kozlov S, Gatei M, et al. ATM-Dependent Phosphorylation of All Three Members of the MRN Complex: From Sensor to Adaptor. Biomolecules, 2015, 5(4): 2877-2902.

[112] Hartlerode A J, Morgan M J, Wu Y, et al. Recruitment and activation of the ATM kinase in the absence of DNA-damage sensors. Nat Struct Mol Biol, 2015, 22(9): 736-743.

[113] Carson C T, Schwartz R A, Stracker T H, et al. The Mre11 complex is required for ATM activation and the G2/M checkpoint. EMBO J, 2003, 22(24): 6610-6620.

[114] Czornak K, Chughtai S, Chrzanowska K H. Mystery of DNA repair: the role of the MRN complex and ATM kinase in DNA damage repair. J Appl Genet, 2008, 49(4): 383-396.

[115] Bai Y, Murnane J P. Telomere instability in a human tumor cell line expressing NBS1 with mutations at sites phosphorylated by ATM. Mol Cancer Res, 2003, 1(14): 1058-1069.

[116] Chiang Y C, Teng S C, Su Y N, et al. c-Myc directly regulates the transcription of the NBS1 gene involved in DNA double-strand break repair. J Biol Chem, 2003, 278(21): 19286-19291.

[117] Zhang Y, Lim C U, Williams E S, et al. NBS1 knockdown by small interfering RNA increases ionizing radiation mutagenesis and telomere association in human cells. Cancer Res, 2005, 65(13): 5544-5553.

[118] Uziel T, Lerenthal Y, Moyal L, et al. Requirement of the MRN complex for ATM activation by

DNA damage. EMBO J, 2003, 22(20): 5612-5621.

[119] Vannier J B, Depeiges A, White C, et al. Two roles for Rad50 in telomere maintenance. EMBO J, 2006, 25(19): 4577-4585.

[120] Robison J G, Dixon K, Bissler J J. Cell cycle-and proteasome-dependent formation of etoposide-induced replication protein A (RPA) or Mre11/Rad50/Nbs1 (MRN) complex repair foci. Cell Cycle, 2007, 6(19): 2399-2407.

[121] Kavitha C V, Choudhary B, Raghavan S C, et al. Differential regulation of MRN (Mre11-Rad50-Nbs1) complex subunits and telomerase activity in cancer cells. Biochem Biophys Res Commun, 2010, 399(4): 575-580.

[122] Compton S A, Choi J H, Cesare A J, et al. Xrcc3 and Nbs1 are required for the production of extrachromosomal telomeric circles in human alternative lengthening of telomere cells. Cancer Res, 2007, 67(4): 1513-1519.

[123] Petroni M, Sardina F, Heil C, et al. The MRN complex is transcriptionally regulated by MYCN during neural cell proliferation to control replication stress. Cell Death Differ, 2015.

[124] Widodo N, Kaur K, Shrestha B G, et al. Selective killing of cancer cells by leaf extract of Ashwagandha: identification of a tumor-inhibitory factor and the first molecular insights to its effect. Clin Cancer Res, 2007, 13(7): 2298-2306.

[125] Jiang W Q, Zhong Z H, Nguyen A, et al. Induction of alternative lengthening of telomeres-associated PML bodies by p53/p21 requires HP1 proteins. J Cell Biol, 2009, 185(5): 797-810.

[126] Yuan J, Yang B M, Zhong Z H, et al. Upregulation of survivin during immortalization of nontransformed human fibroblasts transduced with telomerase reverse transcriptase. Oncogene, 2009, 28(29): 2678-2689.

[127] Kaul Z, Cesare A J, Huschtscha L I, et al. Five dysfunctional telomeres predict onset of senescence in human cells. EMBO Rep, 2012, 13(1): 52-59.

[128] Mender I, Gryaznov S, Dikmen Z G, et al. Induction of telomere dysfunction mediated by the telomerase substrate precursor 6-thio-2'-deoxyguanosine. Cancer Discov, 2015, 5(1): 82-95.

[129] Singh S V, Choi S, Zeng Y, et al. Guggulsterone-induced apoptosis in human prostate cancer cells is caused by reactive oxygen intermediate dependent activation of c-Jun NH2-terminal kinase.

Cancer Res, 2007, 67(15): 7439-7449.

[130] Xiao D, Vogel V, Singh S V. Benzyl isothiocyanate-induced apoptosis in human breast cancer cells is initiated by reactive oxygen species and regulated by Bax and Bak. Mol Cancer Ther, 2006, 5(11): 2931-2945.

[131] Xiao D, Choi S, Johnson D E, et al. Diallyl trisulfide-induced apoptosis in human prostate cancer cells involves c-Jun N-terminal kinase and extracellular-signal regulated kinase-mediated phosphorylation of Bcl-2. Oncogene, 2004, 23(33): 5594-5606.

[132] Stan S D, Hahm E R, Warin R, et al. Withaferin A causes FOXO3a- and Bim-dependent apoptosis and inhibits growth of human breast cancer cells in vivo. Cancer Res, 2008, 68(18): 7661-7669.

[133] Guo X, Deng Y, Lin Y, et al. Dysfunctional telomeres activate an ATM-ATR-dependent DNA damage response to suppress tumorigenesis. EMBO J, 2007, 26(22): 4709-4719.

[134] Stagno D'alcontres M, Mendez-Bermudez A, Foxon J L, et al. Lack of TRF2 in ALT cells causes PML-dependent p53 activation and loss of telomeric DNA. J Cell Biol, 2007, 179(5): 855-867.

[135] Wu G, Jiang X, Lee W H, et al. Assembly of functional ALT-associated promyelocytic leukemia bodies requires Nijmegen Breakage Syndrome 1. Cancer Res, 2003, 63(10): 2589-2595.

[136] Krause D R, Jonnalagadda J C, Gatei M H, et al. Suppression of Tousled-like kinase activity after DNA damage or replication block requires ATM, NBS1 and Chk1. Oncogene, 2003, 22(38): 5927-5937.

[137] Greider C W, Blackburn E H. Identification of a specific telomere terminal transferase activity in Tetrahymena extracts. Cell, 1985, 43(2 Pt 1): 405-413.

[138] Flynn R L, Cox K E, Jeitany M, et al. Alternative lengthening of telomeres renders cancer cells hypersensitive to ATR inhibitors. Science, 2015, 347(6219): 273-277.

[139] Hu J, Hwang S S, Liesa M, et al. Antitelomerase therapy provokes ALT and mitochondrial adaptive mechanisms in cancer. Cell, 2012, 148(4): 651-663.

[140] Hu J, Xu J, Wu Y, et al. Identification of microRNA-93 as a functional dysregulated miRNA in triple-negative breast cancer. Tumour Biol, 2014.

[141] Pignot G, Cizeron-Clairac G, Vacher S, et al. microRNA expression profile in a large series of bladder tumors: identification of a 3-miRNA signature associated with aggressiveness of muscle-

invasive bladder cancer. Int J Cancer, 2013, 132(11): 2479-2491.

[142] Zhang D G, Zheng J N, Pei D S. P53/microRNA-34-induced metabolic regulation: new opportunities in anticancer therapy. Mol Cancer, 2014, 13: 115.

[143] Wadhwa R, Kaul S C, Mitsui Y. Cellular mortality to immortalization: mortalin. Cell Struct Funct, 1994, 19(1): 1-10.

[144] Campisi J. Cancer, aging and cellular senescence. In Vivo, 2000, 14(1): 183-188.

[145] Johnson C, Warmoes M O, Shen X, et al. Epigenetics and cancer metabolism. Cancer Lett, 2015, 356(2 Pt A): 309-314.

[146] Ma X, Choudhury S N, Hua X, et al. Interaction of the oncogenic miR-21 microRNA and the p53 tumor suppressor pathway. Carcinogenesis, 2013, 34(6): 1216-1223.

[147] Tang T, Wong H K, Gu W, et al. MicroRNA-182 plays an onco-miRNA role in cervical cancer. Gynecol Oncol, 2013, 129(1): 199-208.

[148] Zhang J, Sun Q, Zhang Z, et al. Loss of microRNA-143/145 disturbs cellular growth and apoptosis of human epithelial cancers by impairing the MDM2-p53 feedback loop. Oncogene, 2013, 32(1): 61-69.

[149] Glud M, Manfe V, Biskup E, et al. MicroRNA miR-125b induces senescence in human melanoma cells. Melanoma Res, 2011, 21(3): 253-256.

[150] Bai X Y, Ma Y, Ding R, et al. miR-335 and miR-34a Promote renal senescence by suppressing mitochondrial antioxidative enzymes. J Am Soc Nephrol, 2011, 22(7): 1252-1261.

[151] Xiong S W, Lin T X, Xu K W, et al. MicroRNA-335 acts as a candidate tumor suppressor in prostate cancer. Pathol Oncol Res, 2013, 19(3): 529-537.

[152] Gao Y, Zeng F, Wu J Y, et al. MiR-335 inhibits migration of breast cancer cells through targeting oncoprotein c-Met. Tumour Biol, 2014.

[153] Cao J, Cai J, Huang D, et al. miR-335 represents an independent prognostic marker in epithelial ovarian cancer. Am J Clin Pathol, 2014, 141(3): 437-442.

[154] Krell J, Frampton A E, Colombo T, et al. The p53 miRNA interactome and its potential role in the cancer clinic. Epigenomics, 2013, 5(4): 417-428.

[155] Wong M Y, Yu Y, Walsh W R, et al. microRNA-34 family and treatment of cancers with mutant or

wild-type p53 (Review). International Journal of Oncology, 2011, 38(5): 1189-1195.

[156] Rokavec M, Li H, Jiang L, et al. The p53/microRNA connection in gastrointestinal cancer. Clin Exp Gastroenterol, 2014, 7: 395-413.

[157] Scarola M, Schoeftner S, Schneider C, et al. miR-335 directly targets Rb1 (pRb/p105) in a proximal connection to p53-dependent stress response. Cancer Res, 2010, 70(17): 6925-6933.

[158] Schoeftner S, Scarola M, Comisso E, et al. An Oct4-pRb axis, controlled by MiR-335, integrates stem cell self-renewal and cell cycle control. Stem Cells, 2013, 31(4): 717-728.

[159] Dar A A, Majid S, De Semir D, et al. miRNA-205 suppresses melanoma cell proliferation and induces senescence via regulation of E2F1 protein. J Biol Chem, 2011, 286(19): 16606-16614.

[160] Dimri M, Carroll J D, Cho J H, et al. microRNA-141 regulates BMI1 expression and induces senescence in human diploid fibroblasts. Cell Cycle, 2013, 12(22): 3537-3546.

[161] Iqbal N, Mei J, Liu J, et al. miR-34a is essential for p19(Arf)-driven cell cycle arrest. Cell Cycle, 2014, 13(5): 792-800.

[162] Leite K R, Morais D R, Reis S T, et al. MicroRNA 100: a context dependent miRNA in prostate cancer. Clinics (Sao Paulo), 2013, 68(6): 797-802.

[163] Toiyama Y, Okugawa Y, Goel A. DNA methylation and microRNA biomarkers for noninvasive detection of gastric and colorectal cancer. Biochem Biophys Res Commun, 2014, 455(1-2): 43-57.

[164] Suh S O, Chen Y, Zaman M S, et al. MicroRNA-145 is regulated by DNA methylation and p53 gene mutation in prostate cancer. Carcinogenesis, 2011, 32(5): 772-778.

[165] Novello C, Pazzaglia L, Conti A, et al. p53-dependent activation of microRNA-34a in response to etoposide-induced DNA damage in osteosarcoma cell lines not impaired by dominant negative p53 expression. PLoS One, 2014, 9(12): e114757.

[166] Kato Y, Miyaki S, Yokoyama S, et al. Real-time functional imaging for monitoring miR-133 during myogenic differentiation. Int J Biochem Cell Biol, 2009, 41(11): 2225-2231.

[167] Yoon A R, Gao R, Kaul Z, et al. MicroRNA-296 is enriched in cancer cells and downregulates p21WAF1 mRNA expression via interaction with its 3' untranslated region. Nucleic Acids Res, 2011, 39(18): 8078-8091.

[168] Hasan M K, Yaguchi T, Minoda Y, et al. Alternative reading frame protein (ARF)-independent

function of CARF (collaborator of ARF) involves its interactions with p53: evidence for a novel p53-activation pathway and its negative feedback control. Biochem J, 2004, 380(Pt 3): 605-610.

[169] Dohi O, Yasui K, Gen Y, et al. Epigenetic silencing of miR-335 and its host gene MEST in hepatocellular carcinoma. Int J Oncol, 2013, 42(2): 411-418.

[170] Al-Kaabi A, Van Bockel L W, Pothen A J, et al. p16INK4A and p14ARF gene promoter hypermethylation as prognostic biomarker in oral and oropharyngeal squamous cell carcinoma: a review. Dis Markers, 2014, 2014: 260549.

[171] Singh R, Kalra R S, Hasan K, et al. Molecular characterization of collaborator of ARF (CARF) as a DNA damage response and cell cycle checkpoint regulatory protein. Exp Cell Res, 2014, 322(2): 324-334.

[172] Hasan K, Cheung C, Kaul Z, et al. CARF Is a vital dual regulator of cellular senescence and apoptosis. J Biol Chem, 2009, 284(3): 1664-1672.

[173] Cheung C T, Hasan M K, Widodo N, et al. CARF: an emerging regulator of p53 tumor suppressor and senescence pathway. Mech Ageing Dev, 2009, 130(1-2): 18-23.

[174] Cheung C T, Singh R, Kalra R S, et al. Collaborator of ARF (CARF) regulates proliferative fate of human cells by dose-dependent regulation of DNA damage signaling. J Biol Chem, 2014, 289(26): 18258-18269.

[175] Hasan M K, Yaguchi T, Harada J I, et al. CARF (collaborator of ARF) interacts with HDM2: evidence for a novel regulatory feedback regulation of CARF-p53-HDM2-p21WAF1 pathway. Int J Oncol, 2008, 32(3): 663-671.

[176] Kalra R S, Cheung C T, Chaudhary A, et al. CARF (Collaborator of ARF) overexpression in p53-deficient cells promotes carcinogenesis. Mol Oncol, 2015, 9(9): 1877-1889.

[177] Cheung C T, Singh R, Yoon A R, et al. Molecular characterization of apoptosis induced by CARF silencing in human cancer cells. Cell Death Differ, 2011, 18(4): 589-601.